See related commentary on pg 13

NOD2-Induced IκBζ Mediates a Protective Host Response against Epicutaneous *Staphylococcus aureus* Infection

JID Open

Berenice Fischer[1], Antonia Kolb[1], Enrico Focaccia[1], Tanja Kübelbeck[1], Matthias Klein[2,3], Dagmar Löck[1], Francesca Bork[4], Franziska Engelmann[5], Martina Casari[6], Elisa Mazza[1], Carsten Deppermann[3,6], Alexander N.R. Weber[4,7,8,9], Miriam Wittmann[1,3], Birgit Schittek[10], Klaus Schulze-Osthoff[5,7,9] and Daniela Kramer[1,3]

Journal of Investigative Dermatology (2026) **146,** 184–197; doi:10.1016/j.jid.2025.04.036

IκBζ, an atypical and largely unknown member of the IκB family, is a transcriptional coactivator of selective immune functions. In this study, we investigated the role of keratinocyte-derived IκBζ upon infection with a multidrug-resistant *Staphylococcus aureus* strain. Infection of keratinocytes rapidly induced IκBζ expression, leading to an elevated expression of antimicrobial peptides, IL-17/IL-36–responsive genes, and proteins involved in skin barrier function. Conversely, loss of IκBζ resulted in increased *S aureus* internalization, epidermal tissue damage, and severe skin infections in vivo. This impaired host defense upon IκBζ depletion was characterized by reduced antimicrobial peptide expression and diminished recruitment of neutrophils and $CD4^+$ T cells. Importantly, *S aureus*–induced IκBζ expression required the internalization of the bacteria and its sensing by the intracellular receptor NOD2, which triggered IκBζ and its target gene expression. Thus, we identified NOD2–IκBζ signaling as a key pathway mediating a protective host defense against pathogenic *S aureus* infections in the skin.

Keywords: IκBζ, Keratinocytes, *NFKBIZ*, NOD2, *Staphylococcus aureus*

INTRODUCTION

The opportunistic pathogen *Staphylococcus aureus* is a gram-positive skin pathogen that is well-habituated to the human host. An intact skin barrier, a functional antimicrobial immune response, and a balanced skin commensal colonization are prerequisites to prevent epicutaneous *S aureus* infections (Nakatsuji et al, 2016). Skin barrier defects, such as those observed in patients with atopic dermatitis, increase the risk for the development of acute and chronic *S aureus* infections. Moreover, methicillin-resistant strains of *S aureus* have emerged in the last decades, causing significant health issues, such as nonhealing lesions, mild-to-strong skin and soft tissue infections, abscess formation, bacteremia, and sepsis (Del Giudice, 2020). A notable example is the virulent *S aureus* strain USA300, which not only displays increased toxicity due to the expression of several toxins but can also lead to persistent infections due to its increased ability to invade, survive, and proliferate in host cells (Centers for Disease Control and Prevention (CDC), 2003; Miller et al, 2005; Thurlow et al, 2012). The severity of such an infection is highlighted in records from 2019, attributing more than 100,000 deaths across 204 countries to methicillin-resistant strains of *S aureus* (Antimicrobial Resistance Collaborators, 2022). In addition to antibiotic resistance, the expression of various virulence factors, which contribute to enhanced colonization, immune evasion, invasion, and intracellular survival, is believed to promote severe and chronic infections with *S aureus* (Al Kindi et al, 2019; Shoaib et al, 2022). However, the exact underlying molecular mechanisms within the host that determine persistent epicutaneous infections with *S aureus* remain incompletely understood.

Among several receptors being expressed in the skin, keratinocyte-derived toll-like receptor 2 (TLR2) and NOD2 receptor play key roles in sensing *S aureus* infections

[1]*Department of Dermatology, University Medical Center Mainz, Johannes Gutenberg-University, Mainz, Germany;* [2]*Institute of Immunology, University Medical Center Mainz, Johannes Gutenberg-University, Mainz, Germany;* [3]*Research Center for Immunotherapy, University Medical Center Mainz, Johannes Gutenberg-University, Mainz, Germany;* [4]*Institute of Immunology, Department of Innate Immunity, Eberhard Karls-University, Tübingen, Germany;* [5]*Interfaculty Institute for Biochemistry, Eberhard Karls-University, Tübingen, Germany;* [6]*Center for Thrombosis and Hemostasis, University Medical Center Mainz, Johannes Gutenberg-University, Mainz, Germany;* [7]*iFIT – Cluster of Excellence (EXC 2180) "Image-Guided and Functionally Instructed Tumor Therapies", University of Tübingen, Tübingen, Germany;* [8]*CMFI – Cluster of Excellence (EXC 2124) "Controlling Microbes to Fight Infection", University of Tübingen, Tübingen, Germany;* [9]*German Cancer Consortium (DKTK) and German Cancer Research Center (DKFZ) Partner Site, Tübingen, Germany; and* [10]*Department of Dermatology, Eberhard Karls-University, Tübingen, Germany*

Correspondence: Daniela Kramer, Department of Dermatology, University Medical Center Mainz, Johannes-Gutenberg University, Langenbeckstraße 1, Mainz 55131, Germany. E-mail: kramerda@uni-mainz.de

Abbreviations: HiSa, heat-inactivated Staphylococcus aureus; hKC, human primary keratinocyte; KO, knockout; MDP, muramyl dipeptide; TEWL, transepidermal water loss; TLR, toll-like receptor

Received 6 December 2024; revised 6 April 2025; accepted 9 April 2025; accepted manuscript published online 22 May 2025; corrected proof published online 24 June 2025

© 2025 The Authors. Published by Elsevier, Inc. on behalf of the Society for Investigative Dermatology. This is an open access article under the CC BY license (http://creativecommons.org/licenses/by/4.0/).

(Askarian et al, 2018). Both receptors are important for an effective induction of the host defense and subsequent clearance of *S aureus* because natural sequence variations and single nucleotide variations in TLR2 and NOD2 promote reoccurring bacterial infections and chronic diseases related to *S aureus* infections (Kabesch et al, 2003; Lorenz et al, 2000; Macaluso et al, 2007). Moreover, *Tlr2*-knockout (KO) mice are highly susceptible to topical *S aureus* infections (Takeuchi et al, 2000), whereas *Nod2* is critical for the induction of an effective innate immune response against *S aureus* in the skin (Hruz et al, 2009; Roth et al, 2014). Interestingly, however, their relative contribution to the promotion of the cutaneous host defense remains controversial because it seems to vary depending on the depth of infection (colonization, intradermal, or subcutaneous infections) and the staphylococcal strain (Miller et al, 2006; Roth et al, 2014).

The extracellular receptor TLR2 recognizes *S aureus* on the skin by sensing bacteria-derived lipoteichoic acid and lipoproteins (Hashimoto et al, 2006). This recognition activates the transcription factor NF-κB in a MYD88-dependent manner, prompting keratinocytes to express several chemokines (eg, *CXCL8*) and antimicrobial peptides (eg, *DEFB4*, *DEFB103B*) that are needed for an effective host defense (Hanzelmann et al, 2016; Lai et al, 2010). Unlike TLR2, NOD2 receptors are expressed intracellularly, thereby mainly sensing *S aureus* when it invades the cell. NOD2 is activated by binding of bacterial-peptidoglycan fragments, such as muramyl-dipeptide (MDP), or by bacterial RNA, which leads to the activation of NOD2 in a RIG1−MAVS−dependent manner (Grimes et al, 2012; Ngo et al, 2022). Subsequently, NOD2 signaling also activates NF-κB in a RIPK2-dependent manner, leading to the expression of several host defense factors such as antimicrobial peptides, chemokines, and cytokines that subsequently induce the host defense against *S aureus* (Roth et al, 2014; Voss et al, 2006). Thus, TLR2 versus NOD2 activation critically depends on the extracellular or intracellular localization of *S aureus*, whereas the main downstream mediators and effector molecules, such as NF-κB, seem to overlap. Apart from MYD88 in the case of TLR2 and RIPK2 in the case of NOD2, the responsible transcriptional regulators that participate in NOD2 and TLR2 signaling as well as their role in the host defense against epicutaneous *S aureus* infection have not been fully identified yet.

Recent studies, including our own, have shown that IκBζ, encoded by *NFKBIZ*, is an important transcriptional regulator in skin diseases such as psoriasis and presumably also plays a critical role in normal skin processes and homeostasis (Johansen et al, 2015; Kim et al, 2017; Lorscheid et al, 2019; Müller et al, 2018). IκBζ is an atypical nuclear IκB protein, which acts not only as a repressor but, more importantly, can also coactivate a selective subset of NF-κB target genes (Annemann et al, 2016). The mechanism of its differential gene regulation remains largely unknown, but evidence suggests that the transcriptional activity of IκBζ is primarily mediated through chromatin remodeling (Hildebrand et al, 2013; Kayama et al, 2008; Tartey et al, 2014).

In keratinocytes, IκBζ can induce the transcription of a subset of NF-κB target genes encoding several antimicrobial peptides, chemokines, and cytokines (in particular, those involved in IL-17 and IL-36 signaling), which contribute to chronic inflammation when overexpressed (Johansen et al, 2014; Müller et al, 2018). This is also endorsed by the fact that *Nfkbiz*-deficient mice are largely resistant to the induction of psoriatic inflammation (Johansen et al, 2015; Lorscheid et al, 2019). Furthermore, a deficiency of IκBζ is associated with dysbiosis of the skin microbiome and a marked expansion of *S xylosus* and other *Staphylococcus* species (Kim et al, 2017; Terui et al, 2022). So far, however, the physiological functions of IκBζ in the skin, especially its contribution to the barrier function, are largely unexplored.

In this study, we investigated the role of keratinocyte-derived IκBζ in epicutaneous *S aureus* infection. We found that *S aureus* rapidly induced IκBζ expression, requiring the internalization of bacteria into the host cell and activation of the intracellular pattern recognition receptor NOD2. Signaling by NOD2−IκBζ resulted in the induction of antimicrobial peptide genes; chemokines; cytokines involved in IL-17/IL-36 signaling; and importantly, several proteins involved in epidermal barrier function. By contrast, depletion of IκBζ in keratinocytes failed to efficiently activate innate and adaptive immune responses, leading to an increased bacterial colonization, exacerbation of *S aureus* infection, and skin tissue damage. Thus, our data define a previously unknown pathway involving NOD2−IκBζ signaling, which protects the skin against epicutaneous *S aureus* infection.

RESULTS

S aureus–induced IκBζ expression promotes the transcriptional immune response and barrier function of keratinocytes

IκBζ, encoded by the *NFKBIZ* gene, has been identified as an important transcriptional activator of specific NF-κB target genes, including several proinflammatory cytokines and chemokines. Although its function in the skin has mainly been studied as a pathogenic factor in psoriasis, its role in skin infections remains largely unknown. Thus, we analyzed the function of keratinocyte-derived IκBζ during epicutaneous infection with a pathogenic and multidrug-resistant *S aureus* strain of the USA300 lineage (Tenover and Goering, 2009).

We first assessed the effect of *S aureus* infection on the expression of IκBζ in primary human keratinocytes and compared it with the ability of the commensal strain *S epidermidis* to induce IκBζ protein expression using the same multiplicity of infection (multiplicity of infection of 30). Unstimulated keratinocytes did not express IκBζ. Expression of IκBζ protein was however rapidly induced 1 hour after infection with *S aureus* and subsequently declined (Figure 1a). Interestingly, parallel infections with the commensal *S epidermidis* only weakly induced the expression of IκBζ. Next, we depleted IκBζ from human primary keratinocytes (hKCs) using lentiviral expression of an *NFKBIZ*-specific short hairpin RNA (Figure 1b). We investigated transcriptome changes in control and knockdown cells 24 hours after infection with *S aureus*. Interestingly, 919 genes were significantly induced or repressed after infection (cut off: $P \leq .05$, fold change absolute > 2, difference absolute > 3), and approximately 22% of these genes became deregulated in the infected *NFKBIZ*-knockdown cells

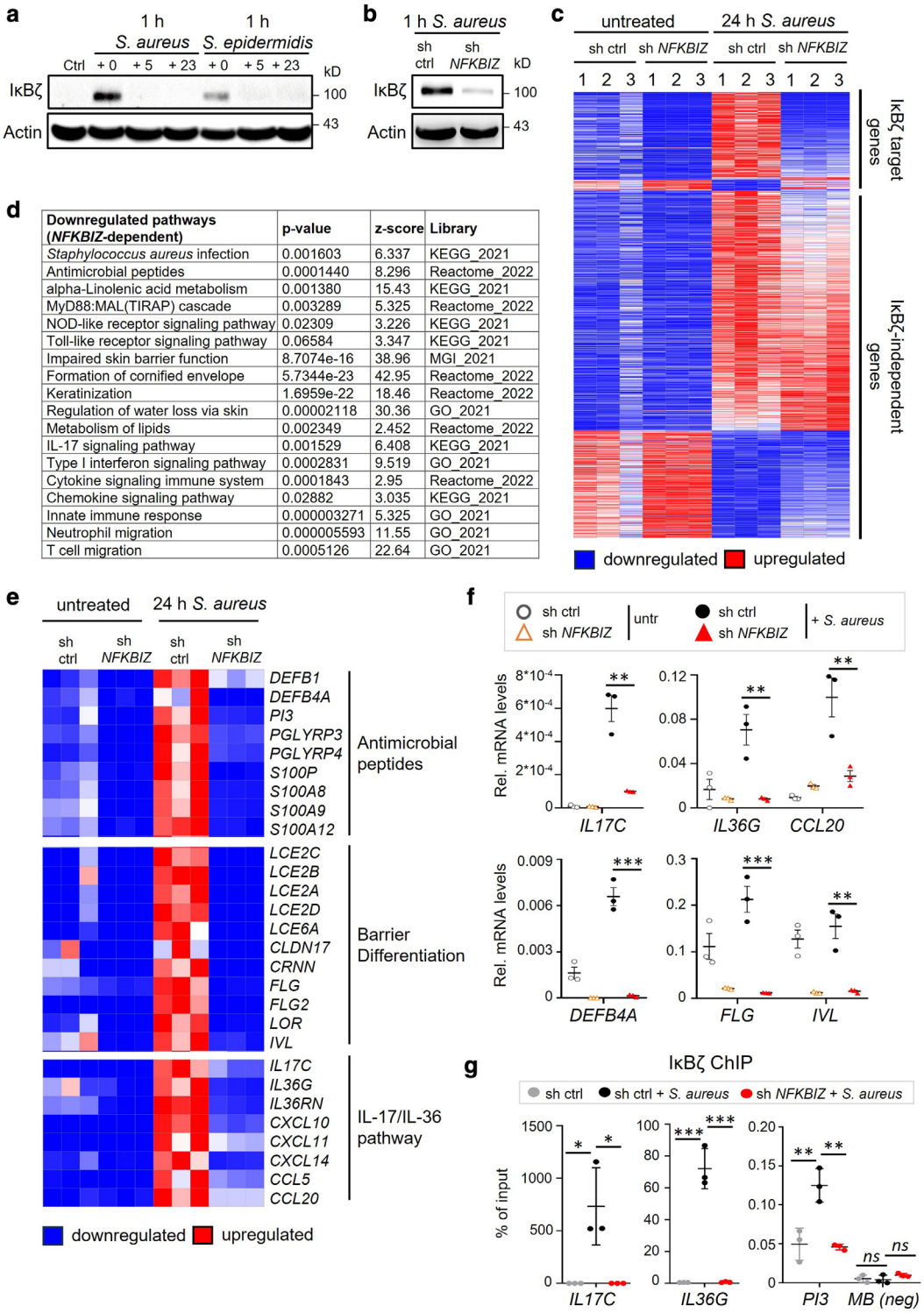

Downregulated pathways (*NFKBIZ*-dependent)	p-value	z-score	Library
Staphylococcus aureus infection	0.001603	6.337	KEGG_2021
Antimicrobial peptides	0.0001440	8.296	Reactome_2022
alpha-Linolenic acid metabolism	0.001380	15.43	KEGG_2021
MyD88:MAL(TIRAP) cascade	0.003289	5.325	Reactome_2022
NOD-like receptor signaling pathway	0.02309	3.226	KEGG_2021
Toll-like receptor signaling pathway	0.06584	3.347	KEGG_2021
Impaired skin barrier function	8.7074e-16	38.96	MGI_2021
Formation of cornified envelope	5.7344e-23	42.95	Reactome_2022
Keratinization	1.6959e-22	18.46	Reactome_2022
Regulation of water loss via skin	0.00002118	30.36	GO_2021
Metabolism of lipids	0.002349	2.452	Reactome_2022
IL-17 signaling pathway	0.001529	6.408	KEGG_2021
Type I interferon signaling pathway	0.0002831	9.519	GO_2021
Cytokine signaling immune system	0.0001843	2.95	Reactome_2022
Chemokine signaling pathway	0.02882	3.035	KEGG_2021
Innate immune response	0.000003271	5.325	GO_2021
Neutrophil migration	0.000005593	11.55	GO_2021
T cell migration	0.0005126	22.64	GO_2021

Figure 1. *S aureus*–dependent induction of IκBζ triggers the expression of genes involved in IL-17 and IL-36 responses, barrier function, and differentiation in keratinocytes. (**a**) Immunoblot analysis of IκBζ in differentiated hKCs treated for 1 h with *S aureus* USA300 or *S epidermidis* (MOI = 30) and further incubated for the indicated times after bacteria removal (0, 5, 23 h). Actin served as a loading control. (**b–f**) RNA-sequencing analysis of *S aureus*–infected primary hKCs with or without *NFKBIZ* depletion. Sample numbers 1–3 indicate 3 independent biological replicates for each group. (**b**) Immunoblot validation of control (sh ctrl) and IκBζ-depleted (sh *NFKBIZ*) hKCs, treated and analyzed as in **a**. (**c**) Heatmap of all genes that were deregulated by *S aureus* infection in control and *NFKBIZ*-knockdown keratinocytes (cut off: $P \leq .05$, fold change absolute > 2, difference absolute > 3). Red indicates upregulation, and blue indicates downregulation. (**d**) GSEA of IκBζ-dependent target genes upon *S aureus* stimulation (from **c**). GSEA analysis was performed with EnrichR. Shown are significantly enriched pathways, sorted by *P*-value. (**e**) Heatmap of selected IκBζ target genes encoding antimicrobial peptides or genes involved in barrier formation, differentiation, or IL-17 and IL-36 signaling. (**f**) Relative mRNA expression levels of IκBζ target genes from control and *NFKBIZ*-deleted primary hKCs, 24 h after *S aureus* infection. For calculation of the relative mRNA levels, values were normalized to the reference gene *RPL37A*. Shown is the mean of 3 biological replicates ± SD. Significance was calculated using a 2-tailed Student's *t*-test (*$P < .05$, **$P < .01$, and ***$P < .001$). (**g**) ChIP of IκBζ or control IgG on

(Figure 1c–e and Supplementary Table S1). Of note, the expression of most of these genes was suppressed by the depletion of *NFKBIZ*, thus validating IκBζ as a transcriptional coactivator in *S aureus*–infected hKCs. Gene set enrichment analysis uncovered that the IκBζ-dependent target genes, which were induced by *S aureus*, mostly comprised antimicrobial peptides, such as defensins (*DEFB4*, *DEFB1*) or S100 proteins (*S100A8*, *S100A9*, *S100A12*), IL-17/IL-36 cytokines (*IL17C*, *IL36G*), and chemokines (*CCL20*, *CXCL10*) (Figure 1d and e and Supplementary Table S1), which we also validated by quantitative PCR (Figure 1f). Moreover, knockdown of IκBζ in *S aureus*–infected cells also significantly inhibited genes orchestrating keratinocyte differentiation, cornified envelope formation, and skin barrier function, including late cornified envelope proteins (*LCE2A-D*), claudin-17 (*CLDN17*), FLGs (*FLG, FLG2*), loricrin, and involucrin (Figure 1f). Of note, similar gene expression changes could be detected in *S aureus*–infected human keratinocytes at an earlier time point upon infection (Supplementary Figure S1a) or in *S aureus*–infected murine control and *Nfkbiz*-KO keratinocytes (Supplementary Figure S1b). Finally, we detected the binding of IκBζ to the promoter regions of its putative target genes, thus validating a direct IκBζ-dependent regulation of its target genes in infected keratinocytes (Figure 1g). Hence, we identified IκBζ as a key factor mediating the host response against *S aureus* infection because it not only promoted IL-17/IL-36 responses but also upregulated the barrier function of keratinocytes, suggestive of an epidermal response that can limit pathogen dissemination.

Deletion of keratinocyte-derived IκBζ in mice results in increased inflammation and tissue damage upon epicutaneous *S aureus* infections

Our in vitro data highlighted that keratinocyte-derived IκBζ is a key factor regulating the host response against *S aureus*. We proceeded to investigate the consequences of a keratinocyte-specific deletion of *Nfkbiz* on spontaneous or experimentally induced *S aureus* skin infection in vivo. For this purpose, we generated keratinocyte-specific *Nfkbiz*-KO mice ($Nfkbiz^{\Delta K14\text{-}cre}$) by crossing floxed *Nfkbiz* mice to K14-cre–expressing strains. Complete deletion of *Nfkbiz* from the epidermal compartment was subsequently validated by detection of IκBζ protein levels in IL-17A and IL-17A/TNF-stimulated control and *Nfkbiz*-KO murine keratinocytes, which were isolated from the tails of the control and $Nfkbiz^{\Delta K14\text{-}cre}$ mice (Supplementary Figure S2a). Interestingly, whereas *Myd88*, *Il17ra*, and *Il17a/Il17f*-KO mice have been reported to suffer from spontaneous skin infections with *S aureus*, leading to the formation of lesions, the skin of $Nfkbiz^{\Delta K14\text{-}cre}$ mice appeared completely healthy, even in aged mice (Supplementary Figure S2b). Moreover, we neither detected any *S aureus* proteins in skin lysates of $Nfkbiz^{\Delta K14\text{-}cre}$ mice (Supplementary Figure S2c), nor could we reveal significant changes in the skin immune homeostasis of those mice (Supplementary Figure S2d and e).

Our following experiments aimed to investigate the consequences of an experimental *S aureus* infection of the skin in $Nfkbiz^{\Delta K14\text{-}cre}$ mice. Of note, application of *S aureus* on the shaved back skin could only induce *Nfkbiz* and inflammatory gene expression in the skin upon a mild skin barrier disruption (Supplementary Figure S2f). Thus, we generated a mild skin barrier defect by tape stripping, before topical infection with *S aureus*. After shaving, depilation, and tape stripping, we soaked small filter paper discs with either PBS (control) or 1×10^8 colony-forming unit *S aureus* USA300 bacteria and placed these filters on the tape-stripped back skin. To prevent unwanted dissemination, oral uptake of the bacteria, or contamination, the back skin of the mice was subsequently covered with dressings and Fixomull. Seven days later, mice were killed and analyzed (Figure 2a). For the overall assessment of local and systemic inflammation, we determined the body weight at the start and end of the treatment, assessed the overall skin barrier defect by measuring the transepidermal water loss (TEWL), and graded *S aureus*–infected skin inflammation with a lesion score (from 0 = healthy appearing skin to 3 = strong skin inflammation) (Figure 2b–d and Supplementary Figure S2g). Of note, PBS-treated control mice also showed a mild loss of body weight and erythematous skin, unrelated to infection but in the context of depilation, tape stripping, and skin dressing. Interestingly, although *S aureus*–infected control ($Nfkbiz^{fl/fl}$) mice also showed signs of skin inflammation, skin infection of $Nfkbiz^{\Delta K14\text{-}cre}$ mice resulted in a significantly higher inflammation score, marked by visible pustules, infiltration, and bright erythema in the area of infected skin (Figure 2b and Supplementary Figure S2g). Concomitantly, infected keratinocyte-specific *Nfkbiz*-KO mice showed significantly worsened defects in the skin barrier (Figure 2c) and greater weight loss than the controls 7 days after infection (Figure 2d). Furthermore, immunohistochemical analysis of the skin of all *S aureus*–infected mice showed signs of skin inflammation, evidenced by epidermal thickening, microabscess formation, and infiltration of immune cells (Figure 2e, top). However, only the skin of infected $Nfkbiz^{\Delta K14\text{-}cre}$ mice displayed a partial loss and increased cell death within the epidermal compartment, as shown by staining for cleaved caspase-3, a marker for apoptosis (Figure 2e, bottom).

Keratinocyte-derived IκBζ mediates the local immune response against epicutaneous *S aureus* infections in mice

We hypothesized that the exacerbated skin lesions in the *S aureus*–infected $Nfkbiz^{\Delta K14\text{-}cre}$ mice were due to a compromised host response, resulting in reduced activation of the innate and adaptive immune response. In line with this hypothesis, flow cytometric analysis of cells isolated from the infected skin revealed a reduced recruitment of neutrophils and monocytes to the infection site in $Nfkbiz^{\Delta K14\text{-}cre}$ mice, together with a severe decrease in ROS production (Figure 3a). Furthermore, whereas *S aureus* infection of control mice resulted in a massive recruitment of $CD4^+$ effector T cells and γδ T cells, deletion of *Nfkbiz* in

promoters of assigned NOD2–IκBζ target genes. Control and *NFKBIZ* knockdown hKCs were infected with *S aureus* for 2 h (MOI = 30). Depicted is the percentage of input of the mean of 3 replicates ± SD. The MB locus served as an internal negative control. ChIP, chromatin immunoprecipitation; GSEA, gene set enrichment analysis; h, hour; hKC, human primary keratinocyte; MB, myoglobulin; MOI, multiplicity of infection.

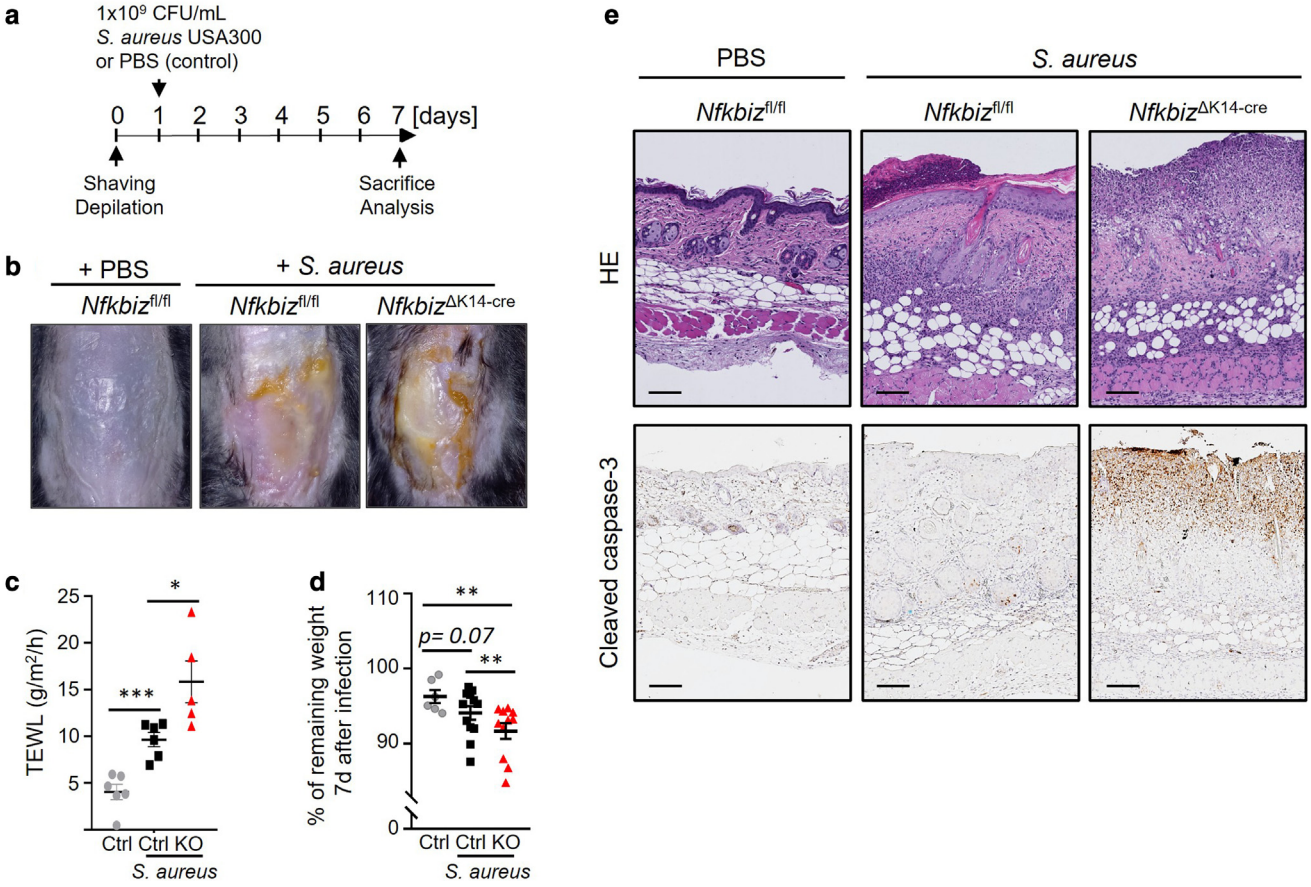

Figure 2. Effects of the deletion of keratinocyte-derived IκBζ on epicutaneous *S aureus* infections in mice. (**a**) Treatment scheme. Mice were shaved and depilated on day 0. On day 1, their back skin was tape stripped immediately before application of either PBS or 1 × 10^8 CFU *S aureus* culture. On day 7, mice were killed and analyzed. (**b**–**d**) Evaluation of *Nfkbiz*$^{fl/fl}$ control mice treated with a PBS control (denoted as Ctrl) and *Nfkbiz*$^{fl/fl}$ or IκBζ-depleted *Nfkbiz*$^{\Delta K14\text{-}cre}$ mice (KO), treated for 7 days with *S aureus*. (**b**) Pictures of the back skin of the mice on day 7. (**c**) Measurement of the TEWL, 7 days after infection (n = 3 mice per group with 1–2 areas of measurement). (**d**) Relative weight loss of the mice. Shown is the relative weight loss at day 7 of each mouse, compared with its weight at the infection starting point. (**e**) FFPE material of back skin was taken at the endpoint on day 7 after infection. Immunohistology was conducted using H&E or cleaved caspase-3 staining. Bars = 100 μm. Significance was calculated using a 2-tailed Student's *t*-test (*$P < .05$, **$P < .01$, and ***$P < .001$). CFU, colony-forming unit; FFPE, formalin-fixed paraffin-embedded; KO, knockout; TEWL, transepidermal water loss.

keratinocytes significantly attenuated the recruitment of T-cell subsets into the infected skin (Figure 3b and c and Supplementary Figure S3a). In conclusion, although the infiltration of immune cells was still visible in the infected skin of *Nfkbiz*$^{\Delta K14\text{-}cre}$ mice, recruitment and activation of important immune cell subsets were significantly impaired upon infection of keratinocyte-specific IκBζ-KO mice. In agreement with these findings and our previously identified IκBζ target genes in *S aureus*–infected keratinocytes, we also detected lower mRNA and protein expression levels of antimicrobial peptides, IL-17/IL-36 cytokines, and their downstream target genes in the skin of *S aureus*–infected *Nfkbiz*$^{\Delta K14\text{-}cre}$ mice (Figure 3d and e and Supplementary Figure S3b). Thus, our in vivo experiments showed that IκBζ is not needed to inhibit *S aureus* colonization and infection; however, once *S aureus* infects the skin, keratinocyte-derived IκBζ expression represents a key factor in promoting immune responses in the skin, thereby limiting tissue damage.

IκBζ inhibits the internalization and dissemination of *S aureus* in vitro and in vivo

We hypothesized that the severe tissue damage in *S aureus*–infected *Nfkbiz*$^{\Delta K14\text{-}cre}$ mice resulted from an impaired host defense, leading to increased internalization, survival, and proliferation of *S aureus*. Therefore, we performed confocal immunofluorescence microscopy of skin sections after 7 days of infection to assess the epidermal bacterial localization. By staining for Protein A of *S aureus* in the infected tissue, a higher bacterial burden was observed in the skin of *S aureus*–infected *Nfkbiz*$^{\Delta K14\text{-}cre}$ mice, accompanied by deeper reaching skin infiltrates, than in the superficial infection with a lower bacterial burden in the control mice (Figure 4a). Thus, our data imply that *S aureus*–mediated induction of IκBζ in the epidermal compartment is needed to induce a protective inflammatory response, which suppresses the deeper dissemination of the pathogen.

Of note, the knockdown of *NFKBIZ* from primary human keratinocytes also resulted in increased internalization of *S aureus* (Figure 4b), possibly owing to an impairment of the outer cell membrane integrity of infected keratinocytes (Supplementary Figure S4). Given the permissive role of skin barrier impairment for *S aureus*–induced *Nfkbiz* expression (Supplementary Figure S2f), we wondered whether bacterial internalization might be a prerequisite for IκBζ induction and a robust immune response. The mechanisms controlling the

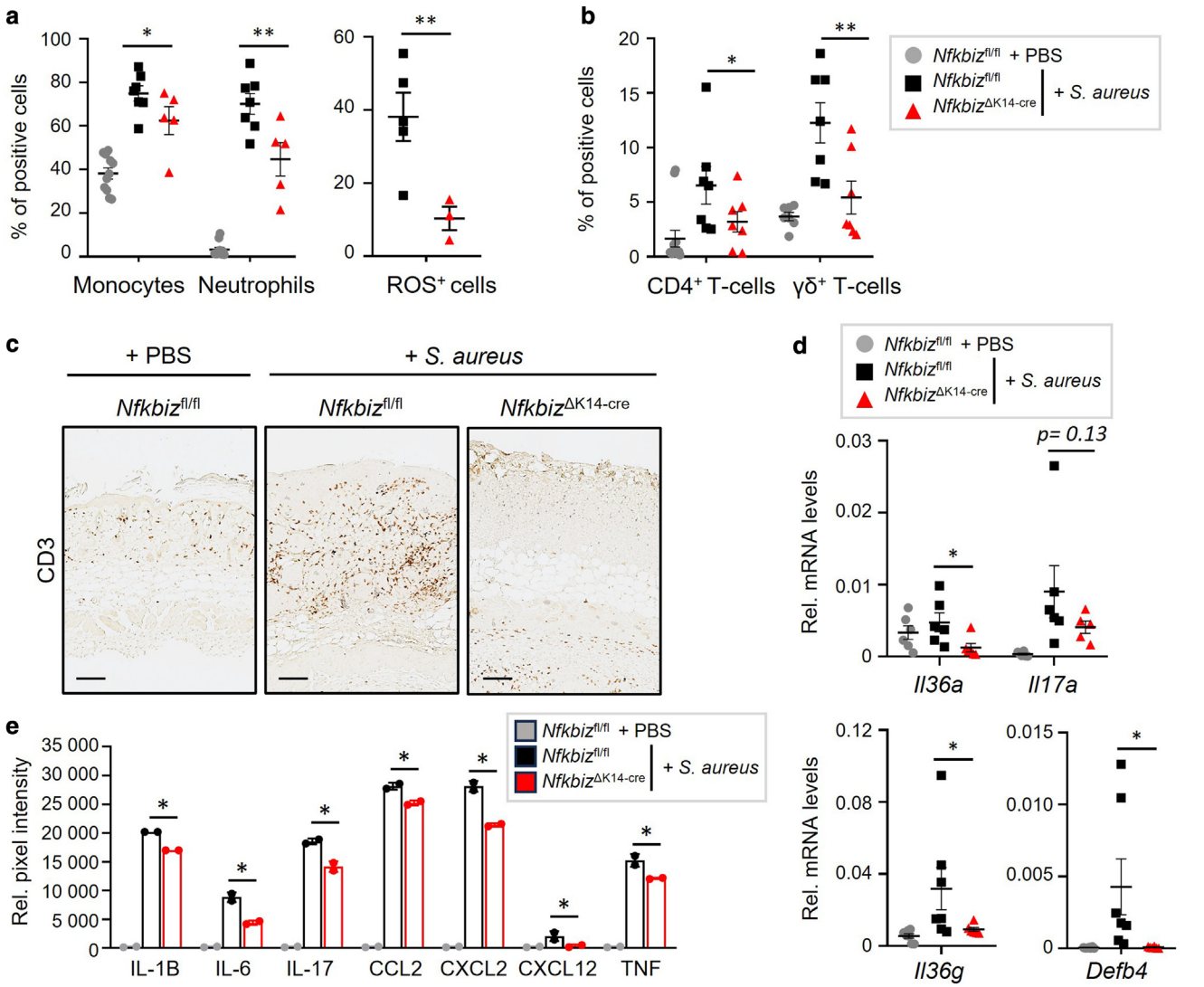

Figure 3. Keratinocyte-derived IκBζ mediates the local immune response against epicutaneous *S aureus* infections in vivo. (**a, b**) Flow cytometric analysis of skin-infiltrating innate immune cells from PBS- and *S aureus*—treated animals at endpoint (n = 5–11 animals per group). (**a**) Relative number of skin-infiltrating neutrophils (Ly6G$^+$), monocytes (Ly6C$^+$), and relative number of ROS-producing granulocytes in the skin. (**b**) Relative number of CD4$^+$ T cells (CD4$^+$ CD25$^-$) and γδ T cells in the skin of PBS- or *S aureus*—treated mice. Shown is the relative percentage of positive cells, after pregating on viable cells. Shown is the mean ± SEM (n = 7–13 mice per group). (**c**) Immunohistochemical staining of infiltrating CD3$^+$ T cells into back skin tissue at the endpoint on day 7 after infection. Bars = 100 μm. (**d**) Gene expression analysis of the skin of *Nfkbiz$^{fl/fl}$* mice treated with PBS (denoted as Ctrl) or *S aureus*—infected *Nfkbiz$^{fl/fl}$* or *Nfkbiz$^{ΔK14\text{-}cre}$* mice, 7 days after infection. Relative mRNA expression was normalized to *Rpl37a*. Shown is the mean ± SEM (n = 5–7 mice per group). (**e**) Cytokine and chemokine levels in the back skin of PBS control or *S aureus*—infected mice at day 7. Protein levels were determined with the Proteome Profiler array using pooled skin lysates from 3 mice per group. Shown are relative pixel values normalized to the average pixel values of all reference spots from each membrane. Significance was calculated using a 2-tailed Student's *t*-test (*$P < .05$, **$P < .01$, and ***$P < .001$).

internalization and intracellular survival of *S aureus* are largely unknown, although the internalization of living bacteria is considered a hallmark of the pathogenicity of certain *S aureus* strains contributing to chronic infections (Al Kindi et al, 2019; Siegmund et al, 2021). To analyze the requirement of bacterial internalization, we performed an infection experiment in primary human keratinocytes in the presence or absence of cytochalasin D, an inhibitor of actin remodeling (Jevon et al, 1999), which completely abolished the internalization of *S aureus* (Figure 4c). In line with our hypothesis that internalization triggers IκBζ expression, application of cytochalasin D partially suppressed *S aureus*—mediated induction of IκBζ and its target gene expression (Figure 4d and e). Moreover, we performed a side-by-side infection experiment using both living and heat-inactivated *S aureus* (HiSa) cultures in primary human keratinocytes because heat-inactivation of *S aureus* is known to block internalization (Ngo et al, 2022). We found that HiSa failed to induce IκBζ protein expression (Figure 4f) and subsequent IκBζ target gene expression (Figure 4g), although the expression of IκBζ-independent NF-κB target genes, such as *NFKBIA* or *ICAM1*, was equally induced upon treatment with living bacteria or HiSa. Together, these experiments show that the internalization of *S aureus* seems to be a key event promoting IκBζ induction and subsequent inflammatory responses.

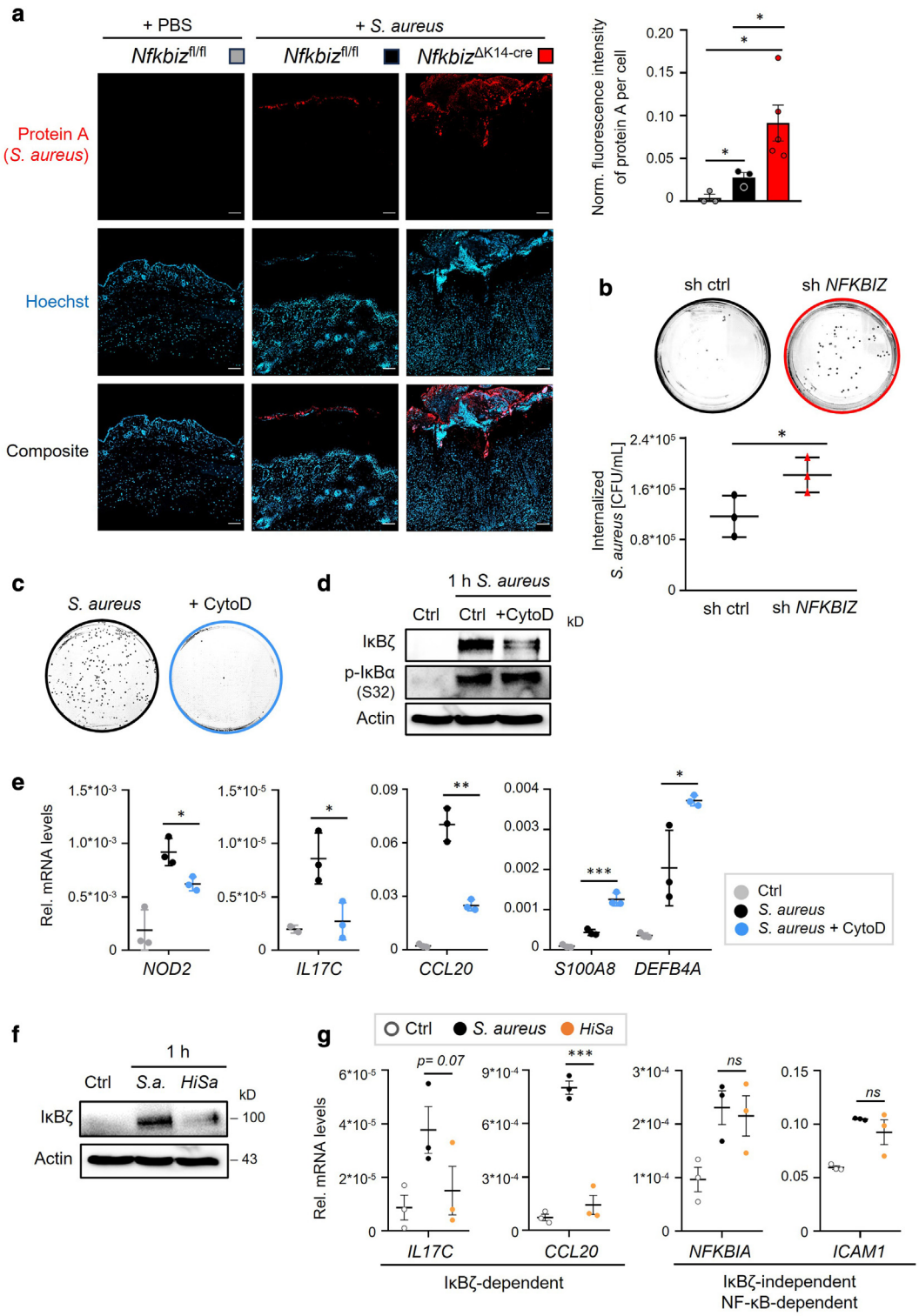

Figure 4. IκBζ inhibits the internalization and dissemination of *S aureus* in vitro and in vivo. (**a**) Immunofluorescence staining of FFPE samples from the back skin of PBS control mice and infected *Nfkbiz*$^{fl/fl}$ (Ctrl) or *Nfkbiz*$^{\Delta K14\text{-}cre}$ (KO) mice, 7 days after infection. Left site: internalized *S aureus* bacteria were detected by staining with an anti−Protein A antibody (red). Hoechst dye was used for nuclear DNA staining (blue). Bars = 100 μm. Right site: fluorescence intensity was normalized to the amount of protein A per cell after the intensity of Hoechst staining was equated to the PBS control mouse. The bar diagram shows data from n = 3−4 mice per group. (**b**) Relative internalized *S aureus* CFUs per ml in control or *NFKBIZ*-depleted primary hKCs. Cells were infected for 1 h with MOI = 30, washed, and incubated for additional 23 h in the presence of antibiotics to kill external bacteria. hKCs were trypsinized, washed, and lysed in 0.1% Triton-X-100 for 1 h at RT before the suspension was plated at different dilutions on agar plates and incubated overnight at 37 °C. Depicted are recovered CFUs from 2 individual experiments. (**c**) Representative pictures of the relative amount of internalized *S aureus* after infection of human keratinocytes in the presence or absence of 0.5 μM CytoD. Cells were infected for 1 h with MOI = 30, washed, and incubated for an additional 23 h in the presence of antibiotics to kill external bacteria. (**d**) IκBζ protein levels in differentiated primary human keratinocytes, left untreated or infected with *S aureus* (MOI = 30) for 1 h in the presence or absence of 0.5 μM CytoD. Actin served as a loading control. (**e**) Gene expression analysis of human keratinocytes, treated as in **d** but after an additional

NOD2 but not TLR2 signaling induces IκBζ expression and its target gene expression in *S aureus*–infected keratinocytes

Subsequently, we wanted to better understand the upstream signaling that triggers IκBζ expression in *S aureus*–infected keratinocytes. Two receptors, TLR2 and NOD2, have been reported as the main receptors mediating immune responses upon cutaneous *S aureus* infections in mice (Hruz et al, 2009; Takeuchi et al, 2000). Interestingly, although both receptors can activate NF-κB signaling, the main difference between these 2 receptors derives from their extracellular (TLR2) and intracellular (NOD2) localization (Figure 5a). On the basis of our results that internalization of *S aureus* is a prerequisite for IκBζ induction in keratinocytes, we hypothesized that NOD2 but not TLR2 is needed to trigger IκBζ protein expression.

To test this hypothesis, we first investigated whether both signaling pathways can induce IκBζ expression in primary human keratinocytes. To this end, NOD2 signaling was activated by stimulating cells with MDP, a specific NOD2 agonist, whereas Pam3CSK4 was applied to activate TLR1/2 signaling (Figure 5b). As expected, both ligands could induce IκBζ expression (Figure 5b). Next, we analyzed *S aureus*–induced IκBζ expression in hKCs after blockade of either NOD2 or TLR2. To inhibit NOD2 signaling, we applied GSK583, an inhibitor of RIPK2, which is a specific adaptor kinase downstream of NOD1/2 (Figure 5a). TLR2 signaling was abrogated using the small-molecule inhibitor TL2-C29 (Figure 5c and Supplementary Figure S5a). Comparable infection rates for all treatment groups were verified by immunoblot analysis of IκBα phosphorylation. Intriguingly, we revealed that only inhibition of NOD2 signaling was able to suppress *S aureus*–induced IκBζ and its target gene expression (Figure 5c [left] and Supplementary Figure S5b). Conversely, inhibition of TLR2 did not affect the expression of IκBζ and, partially, even elevated IκBζ target gene expression in *S aureus*–infected cells (Figure 5c [right] and Supplementary Figure S5a). Thus, NOD2 rather than TLR2 signaling induces IκBζ in *S aureus*–infected keratinocytes.

Because IκBζ has not been described as a downstream mediator of NOD2 signaling so far, we sought to better define its molecular function downstream of NOD2. For this purpose, control and *NFKBIZ*-depleted primary human keratinocytes were stimulated with the NOD2 agonist MDP for 24 hours, followed by transcriptome analysis to identify NOD2- and IκBζ-dependent target genes (Figure 5d). RNA sequencing showed that MDP stimulation significantly modulated the expression of 379 genes, with approximately 32% of the NOD2-dependent genes being either repressed and 5.5% being induced in the MDP-treated *NFKBIZ* knockdown cells. Importantly, about 34% of these NOD2-IκBζ target genes were similarly affected by *NFKBIZ* knockdown in *S aureus*–infected keratinocytes. The finding that genes encoding antimicrobial peptides and IL-17/IL-36–responsive genes were particularly affected is consistent with our observations in *S aureus*–infected *NFKBIZ*-knockdown keratinocytes (Figure 5e and Supplementary Figures S5c and S6 and Supplementary Table S2). In line with these results, IκBζ target genes downstream of NOD2 could also be validated in MDP-stimulated control and *Nfkbiz*-KO murine keratinocytes (Supplementary Figure S5d). Moreover, in agreement with the effect of *NFKBIZ* depletion, NOD2 inhibition also increased the overall internalization and survival of *S aureus* in hKCs (Figure 5f). Finally, we tested whether exogenous overexpression of IκBζ could partially overcome the effects of RIPK2 inhibition in *S aureus*–infected keratinocytes. For this purpose, we lentivirally overexpressed IκBζ and re-exposed the cells to *S aureus* infection in the presence or absence of active NOD2 signaling using the previously validated RIPK2 inhibitor. Notably, overexpression of IκBζ could efficiently counteract the effects of RIPK2 inhibition in *S aureus*–infected keratinocytes (Figure 5g and h). Together, these findings highlight IκBζ as a key downstream mediator of NOD2 responses in keratinocytes.

DISCUSSION

Recent studies have identified keratinocyte-derived IκBζ as a critical transcriptional regulator in the pathogenesis of psoriasis and in maintaining skin microbiota homeostasis (Johansen et al, 2015; Kim et al, 2017; Lorscheid et al, 2019; Terui et al, 2022). However, the function of IκBζ during skin infections and host defense is largely unexplored. Our study revealed that *S aureus* infection of keratinocytes rapidly induced IκBζ, leading to the induction of various host defense factors, including antimicrobial peptides, cytokines, and chemokines. Importantly, we found the induction of IκBζ expression upon *S aureus* infection was far more pronounced than upon infection with the commensal and coagulase-negative strain *S epidermidis*. Consequently, we observed a higher internalization rate of *S aureus* into *NFKBIZ*-knockdown keratinocytes, consistent with previous findings underscoring the importance of antimicrobial peptides in controlling *S aureus* colonization (Braff et al, 2005; Ong et al, 2002; Simanski et al, 2010). IκBζ expression in *S aureus*–infected cells also upregulated several genes involved in the formation of the cornified envelope, suggesting a previously unrecognized role of IκBζ in maintaining the skin barrier. In agreement, we could validate an impaired skin barrier in IκBζ-deleted keratinocytes and skin, for example, using TEWL measurement among other methods. The disturbance of the epidermal barrier represents a critical factor for switching skin colonization with *S aureus* to infection, as seen in patients with atopic dermatitis (Nakatsuji et al, 2016). The loss of the epidermal barrier in the keratinocyte-specific IκBζ-KO mice might explain the deeper skin penetration of *S aureus*, whereas infections in control mice remained superficial. Future studies should investigate the extent to which different clinical isolates of

incubation time of 23 h, after an initial infection for 1 h. (**f**) IκBζ protein levels in differentiated primary hKCs infected with either living or HiSa cultures for 1 h (MOI = 30). Actin served as a loading control. (**g**) Gene expression analysis of *S aureus* (MOI = 30) or HiSa-infected cells 24 h after infection, divided into IκBζ-dependent and IκBζ-independent NF-κB target genes. Relative mRNA levels were normalized to the reference gene *RPL37A*. Shown is the mean of 3 biological replicates ± SD. Significance was calculated using a 2-tailed Student's *t*-test (*$P < .05$, **$P < .01$, and ***$P < .001$). CFU, colony forming unit; CytoD, cytochalasin D; FFPE, formalin-fixed paraffin-embedded; HiSa, heat-inactivated *S aureus*; h, hour; hKC, human primary keratinocyte; KO, knockout; MOI, multiplicity of infection; RT, room temperature.

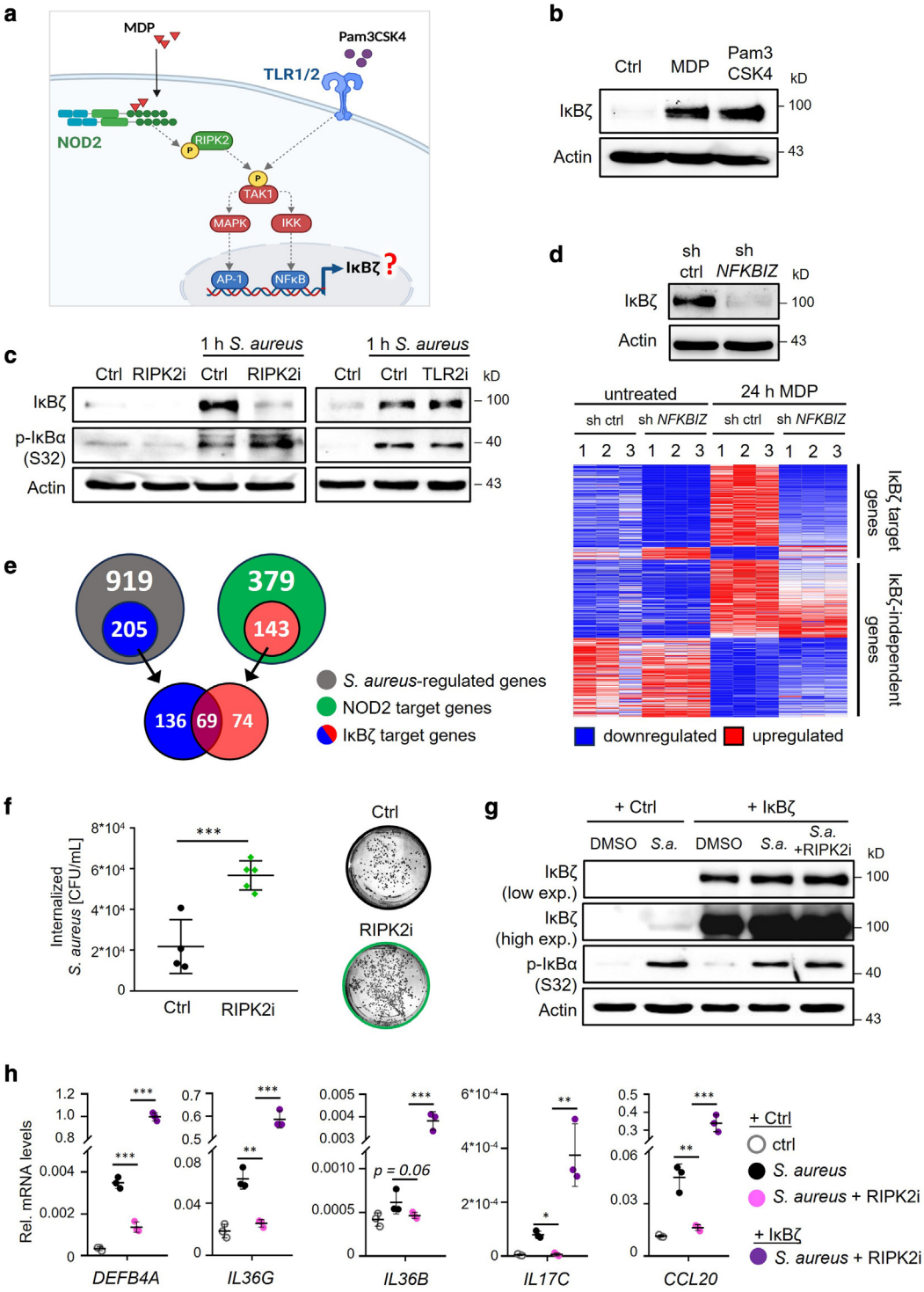

Figure 5. *S aureus*–mediated activation of NOD2 signaling induces IκBζ and its target gene expression in keratinocytes. (**a**) Scheme of TLR2 and NOD2 signaling pathways in keratinocytes. (**b**) Immunoblot analysis and relative mRNA levels of IκBζ in keratinocytes stimulated with NOD2 (MDP) and TLR2 (Pam3CSK4) agonists. Differentiated hKCs were treated for 1 h with 20 μg/ml MDP together with ProteoJuice transfection reagent or with 10 μg/ml Pam3CSK4. Actin served as a loading control. (**c**) IκBζ protein levels in differentiated hKCs infected with *S aureus* (1 h, MOI = 30), in the presence or absence of RIPK2 inhibitor GSK583 (5 μM) or TLR2 inhibitor TL2-C29 (50 μM). Phosphorylated IκBα (S32) was used to control for effective infection with *S aureus*. Actin served as a loading control. (**d**) Heatmap of all MDP-responsive genes that were induced or repressed in control or *NFKBIZ*-depleted hKCs 24 h after stimulation with 20 μg/ml MDP in the presence of ProteoJuice (cut off: $P \leq .05$, fold change absolute > 2, difference absolute > 3). Blue indicates downregulated gene expression; red indicates upregulated gene expression. (**e**) Overlap of significantly regulated, IκBζ-dependent target genes in *S aureus*–infected (gray) or MDP-treated (green) cells. The overlap comprises 69 genes (details also presented in Supplementary Figures S5c and S6). (**f**) Relative internalized *S aureus* CFU per ml in control (left) or RIPK2 inhibitor–treated hKCs (right). Cells were starved overnight in the absence or presence of RIPK2i (GSK583, 1 μM), infected for 1 h with MOI = 30, washed, and incubated further for 23 h in the presence of fresh RIPK2i and antibiotics to kill external bacteria. hKCs were trypsinized, washed, and lysed in 0.1% Triton-X-100 for 1 h at RT before the suspension was plated in different dilutions on agar plates and incubated overnight at 37 °C. (**g**) Validation of IκBζ overexpression in *S aureus*–infected and RIPK2i-treated hKCs. Phosphorylation levels of IκBα (S32) control equal *S aureus* infection. Actin served as a

staphylococcal strains, especially from patients with atopic dermatitis, can induce or repress IκBζ expression, thereby modulating skin barrier defects and disease severity in atopic dermatitis.

Previously, IL-36 has been identified as a key mediator in the recruitment and activation of neutrophils and T cells upon epicutaneous *S aureus* infection (Liu et al, 2017). We discovered that *S aureus*—mediated expression of IL-36 cytokines critically depends on keratinocyte-derived IκBζ expression in vivo and in vitro, similar to previous findings in psoriasis (Müller et al, 2018). Thus, downregulation of IL-36 signaling might explain the compromised host defense and the impaired recruitment and activation of neutrophils and T cells in the keratinocyte-specific *Nfkbiz*-KO mice.

Importantly, despite the essential role of keratinocyte-derived IκBζ in promoting an effective host defense against *S aureus* infection, $Nfkbiz^{\Delta K14\text{-}cre}$ mice did not exhibit spontaneous *S aureus* infections and appeared normal (Lorscheid et al, 2019). This was unexpected because the global or keratinocyte-specific deletion of known upstream regulators of IκBζ, such as IL-17A/IL-17F or MYD88 (Johansen et al, 2014; Müller et al, 2018; Yamamoto et al, 2004), resulted in spontaneous *S aureus* infections in mice (Moos et al, 2023; Takeuchi et al, 2000). This prompted us to investigate the mechanism of how IκBζ expression is induced upon epicutaneous *S aureus* infections and whether the mere exposure or colonization with *S aureus* is already sufficient to induce IκBζ expression. Of note, the molecular mechanism leading to *S aureus* internalization into keratinocytes is incompletely understood. Therefore, we indirectly blocked the internalization of *S aureus* by applying the actin-remodeling agent cytochalasin D or HiSa, both of which were shown to suppress *S aureus* internalization into keratinocytes (Ngo et al, 2022). Surprisingly, we revealed that the internalization of bacteria and the subsequent activation of the intracellular NOD2 receptor were mandatory for the induction of IκBζ expression in keratinocytes. Consistent with these results, *Nod2*-KO mice also failed to show spontaneous *S aureus* infections (Stroo et al, 2012; Williams et al, 2017), whereas deletion of *Myd88*, a downstream factor of TLR2 and IL-1 signaling, resulted in increased spontaneous infections with *Staphylococci* strains and the formation of skin lesions (Tartey et al, 2014). Moreover, IL-36γ, an IκBζ target gene in *S aureus*—infected cells, was only expressed upon skin exposure to pathogenic bacterial strains (Macleod et al, 2020). Thus, all 3 molecules—NOD2, IκBζ, and IL-36γ—represent key factors that trigger the host defense only upon invasion of pathogenic *S aureus* strains rather than during mere skin colonization.

Surprisingly, TLR2 inhibition did not modify IκBζ expression in *S aureus*—infected cells, although TLR2 ligands can induce IκBζ. This might be caused by the fact that TLR2 is primarily involved in controlling *S aureus* colonization and proliferation extracellularly, whereas NOD2 plays a key role in restricting *S aureus* infections after internalization. Differentiated keratinocytes are continuously exposed to bacteria and their TLR ligands. We propose that TLR2 activation in differentiated keratinocytes is dampened to avoid IκBζ-dependent immune responses, which could otherwise lead to the clearance of commensals or elicit autoinflammation, as observed in psoriasis (Johansen et al, 2015; Müller et al, 2018). Conversely, pathogens that can internalize into keratinocytes, thereby escaping clearance by antimicrobial peptides or phagocytosis, induce NOD2 and IκBζ expression, leading to a full-blown immune response.

Because *NOD2* polymorphisms and loss-of-function mutations have been implicated in other pathologies, dysregulated IκBζ expression could also contribute to diseases such as Crohn's or chronic granulomatous disease (Negroni et al, 2018; Ogura et al, 2001; Sidiq et al, 2016). In addition, aberrant expression of IκBζ might be involved in atopic dermatitis, in which genetic variations of *NOD2* have been linked not only to the skin pathology (Kabesch et al, 2003; Macaluso et al, 2007) but also to aberrant T helper 2 responses (Gimenez-Rivera et al, 2023; Jiao et al, 2016). It will be of special interest to investigate whether this, to our knowledge, previously unrecognized function of IκBζ in the regulation of barrier functions contributes to NOD2-dependent pathologies, such as inflammatory bowel disease or atopic dermatitis.

In conclusion, our data reveal a critical role of the hitherto unrecognized NOD2—IκBζ axis in the protective host defense against cutaneous *S aureus* infections. Given that overexpression of IκBζ has been identified as a key driver in autoinflammatory gene expression, balancing the epidermal IκBζ expression appears to be essential to maintain a healthy skin homeostasis.

MATERIALS AND METHODS

Isolation, cultivation, and stimulation of differentiated human keratinocytes from foreskin

hKCs were freshly isolated from foreskin as described (Müller et al, 2020). For differentiation of the keratinocytes, cells were seeded and differentiated for 72 hours in the presence of 2 mM calcium chloride in supplemented CnT-07 epithelial proliferation medium (catalog CnT-07, CELLnTEC). Before stimulation, cells were starved overnight in nonsupplemented CnT-07 medium, without calcium chloride or antibiotics. For stimulation with TLR1/2 and NOD2 ligands, pre-starved cells were treated for 1 hour with 10 μg/ml TLR1/2 ligand Pam3CSK4 (catalog tlrl-pms, InvivoGen) or transduced with MDP (active L-D isomer, catalog tlrl-mdp, InvivoGen) using 2.5 μl ProteoJuice Protein Transfection reagent (catalog 71281-3, Novagen) in nonsupplemented medium for 20 minutes at room temperature. For RIPK2 inhibition, 1 μM or 5 μM GSK583 (catalog S8261, Selleckchem) was added at the time point of starvation and kept on the cells during the complete treatment time. The following inhibitors (all dissolved in DMSO) were applied 1—2 hours in advance before infection and kept on the cells during the complete treatment

loading control. Cells were infected for 1 h with *S aureus* (MOI = 30) in the presence or absence of 5 μM RIPK2i GSK583. (**h**) Relative mRNA expression levels of IκBζ target genes from control and *NFKBIZ*-overexpressing primary hKCs 24 h after *S aureus* infection in the presence or absence of 5 μM RIPK2i GSK583. Cells were infected as in **f**. Values were normalized to the reference gene *RPL37A*. Shown is the mean of 3 biological replicates ± SD. Significance was calculated using a 2-tailed Student's *t*-test (*$P < .05$, **$P < .01$, and ***$P < .001$). CFU, colony forming unit; h, hour; hKC, human primary keratinocyte; MDP, muramyl dipeptide; MOI, multiplicity of infection; RIPK2i, RIPK2 inhibitor; RT, room temperature; TLR2, toll-like receptor 2.

time—TLR2 inhibition: 50 μM TLR2i (catalog TL2-C29, Invivogen) and block of internalization: 0.5 μM cytochalasin D (catalog 11330-1, Cayman Chemical).

S aureus cultivation and propagation

Methicillin-resistant *S aureus* strain USA300 wild-type LAC was kindly provided by Bernhard Krismer (Eberhard Karls-University, Tübingen, Germany), and bacteria stocks of the commensal *S epidermidis* stock were kindly provided by Birgit Schittek (Eberhard Karls-University, Tübingen, Germany). For infection experiments, *S aureus* overnight cultures were inoculated from live material plated on tryptic soy broth agar plates and cultivated in an orbital shaking incubator at 37 °C. The next day, cultures were inoculated using a 1:100 dilution from the overnight culture. Incubation was performed until the bacteria reached their log-growth phase for optimal infection efficiency, as determined by measuring the optical density at 600 nm. After centrifugation (4000 r.p.m., 5 minutes at 4 °C), the bacteria pellet was washed with PBS, centrifuged again, and resuspended in the respective medium (PBS for mice experiments or basal CnT-07 medium for hKCs). Again, measurement at optical density at 600 nm was conducted to determine the final concentration of bacteria. For in vitro infection with live bacteria, a multiplicity of infection of 30 was calculated. Likewise, the same volume of USA300 wild-type bacteria was used to generate HiSa cultures, which were obtained by boiling for 1 hour at 90 °C before freezing for at least 4 hours at −20 °C.

S aureus infection of keratinocytes and internalization assays

Starved, differentiated hKCs or murine primary keratinocytes were infected with a multiplicity of infection of 30 of *S aureus* USA300 for 1 hour at 37 °C, followed by 2 washing steps using PBS. Cells were either harvested directly for immunoblot analysis or further incubated for 23 hours at 37 °C in a humidified atmosphere with 5% carbon dioxide using basal keratinocyte media without supplements but in the presence of the respective antibiotics to kill external bacteria. To assess bacterial internalization into hKCs, infected cells were washed twice with PBS 23 hours after infection and trypsinized for 15 minutes at 37 °C before the reaction was stopped with DMEM (supplemented with 10% fecal calf serum). The cell suspension was centrifuged, once washed with PBS (1000 r.p.m., 5 minutes), and resuspended in 1 ml 0.1% Triton-X-100. Mild lysis was conducted for 1 hour at room temperature before 20 μl were plated on tryptic soy broth agar plates and incubated at 37 °C for approximately 15 hours. The next day, colony-forming units were recorded.

Generation of *NFKBIZ* knockdown or overexpression cells

Lentiviral particles were produced in human embryonic kidney 293T cells through lipofectamine 2000 transfection of the VSV-G envelope–expressing vector pMD2.G (catalog 12259, Addgene), a second-generation packaging plasmid psPAX2 (catalog 12260, Addgene), and either an empty pLKO.1-puro plasmid as control (catalog 8453, Addgene) or pLKO.1-TRCN0000147551 encoding for short hairpin RNA against *NFKBIZ*. For the generation of overexpression cells, the same packaging plasmids together with either an empty mammalian expression vector pRDI292 as a control (+ Ctrl) or Flag-tagged *NFKBIZ* overexpression plasmid (+ IκBζ) cloned into pRDI292 were transfected (plasmids were provided by Stephan Hailfinger, University Medical Center Münster, Germany). Afterward, hKCs were transduced with lentivirus in the presence of 10 μg/ml polybrene (catalog TR-1003-G, Sigma-Aldrich), followed by puromycin selection (1 ng/ml, catalog ant-pr, InvivoGen) over time.

Mouse experiments

All animal experiments were approved by the local animal ethics committee (G22-1-049, Landesuntersuchungsamt Rheinland-Pfalz) and conducted following German law and guidelines for animal care. For all in vivo experiments, both male and female mice at an age between 8 to 12 weeks were used. B6.Cg.Nfkbiz<tm1.1Muta> mice were used as control mice (called $Nfkbiz^{fl/fl}$), whereas keratinocyte-specific depletion of *Nfkbiz* was investigated using the previously generated and described mouse strain B6.Cg.Nfkbiz<tm1.1Muta> Tg(KRT14-cre)/Tarc (called $Nfkbiz^{\Delta K14\text{-}cre}$) (Lorscheid et al, 2019). Starting 1 day before infection, the entire back skin of all mice was shaved and depilated using shaving cream. The next day, the back skin was tape stripped 8 times to create a mild barrier defect. Afterward, 2 sterile filter discs soaked with either PBS or 1×10^8 colony-forming unit *S aureus* were placed on the back skin of each mouse, followed by the coverage of the area using a plaster and Fixomull to avoid contamination. On day 7, all mice were killed, and the covering was removed and subsequently analyzed in parallel. After removal of the covering and filter discs, the severity of skin inflammation was assessed using the following score, which was adapted from a previous publication assessing the relative grade of erythema, edema, scaling, and erosion (Patrick et al, 2021): 0 = healthy-appearing skin, 0.5 = scaling, 1 = scaling with mild local infection (erythema), 2 = moderate epicutaneous infection affecting <50% of back skin, and 3= strong epicutaneous infection with erosion, pus, and abscess formation, affecting the whole area.

Assessment of TEWL in mice

TEWL was measured on day 7 after infection within the area where *S aureus* had been topically applied. Measurements were taken as soon as the mice had been killed and the bandages and filter discs removed. TEWL was assessed using the Tewameter TM300 device (Courage & Khazaka, Cologne, Germany), which employs the open-chamber method to continuously measure water evaporation without disrupting the skin's microenvironment. The probe of the device provided an indirect measurement of the water vapor density gradient, whereas a microprocessor analyzed the data and expressed the evaporation rate in $g/h/m^2$. During the measurement, the room temperature was consistently maintained at 21.0 °C. TEWL was recorded at 2 independent skin sites per mouse.

Isolation and treatment of murine keratinocytes from mouse tails

Murine primary keratinocytes were isolated from mouse tails as previously described (Fischer et al, 2023). For the analysis of *Nfkbiz*-KO mouse keratinocytes, we isolated murine primary keratinocytes from the tails of $Nfkbiz^{\Delta K14\text{-}cre}$ and $Nfkbiz^{fl/fl}$ (B6.Cg.Nfkbiz<tm1.1Muta>) mice.

RNA extraction and gene expression analysis by qPCR

All gene expression analyses were conducted as previously published (Müller et al, 2018). For calculation of the relative mRNA levels, Ct values were normalized to a housekeeping gene (*RPL37A* or *U6RNA* for human samples, *Rpl37*a or *Actb* for murine samples) using the $2^{-\Delta Ct}$ method. Primer sequences are found in Supplementary Tables S3 and S4.

RNA sequencing and analysis

For transcriptome analysis, both sequencing and library construction from total RNA were performed by Novogene (Munich, Germany). Barcoded mRNA sequencing libraries were prepared from 200 ng total RNA using polyA-tailed mRNA enrichment. Final libraries were

checked with Qubit 2.0 and real-time PCR for quantification and bioanalyzer Agilent 2100 for size-distribution detection. Quantified libraries were sequenced on Illumina Novaseq 6000 platform, according to effective library concentration and data amount. Sequencing strategy was paired-end 150 cycles. CLC Genomics workbench (version 24.0, Qiagen) was used for further processing of the sequencing raw reads. Mapping against the human reference genome hg38 (GRCh38.109) was performed by the Next-Generation Sequencing Core Facility (Research Center for Immunotherapy) using CLC's default settings (mismatch cost = 2, insertion cost = 3, deletion cost = 3, length fraction = 0.8, similarity fraction = 0.8, global alignment = no, strand specific = both, library type = bulk, maximum number of hits for a read = 10, count paired reads as 2 = no, and ignore broken pairs = yes). Differentially expressed genes were filtered for a minimum absolute fold change > 2 with a difference cut off of absolute > 3 between untreated and treated cells of each cell line. Significant regulation was observed in genes of an adjusted $P \leq .05$. Raw data of the gene expression datasets presented in this study were published under the Gene Expression Omnibus accession number GSE267665 (details are provided in Data Availability Statement). Heatmaps were generated using Morpheus software (Morpheus, https://software.broadinstitute.org/morpheus), and pathway enrichment analysis and comparison between regulated gene sets were conducted using EnrichR (Evangelista et al, 2023).

Immunoblot analysis

Immunoblot analysis was performed as described (Müller et al, 2018). The following antibodies were used (all from Cell Signaling Technology): anti-IκBζ (catalog 9244), anti−p-IκBα (S32) (catalog 2859), and anti−β-Actin (catalog 3700). HSC70 antibody was purchased from Santa Cruz Biotechnology (catalog Sc-7298), and antiserum against *S aureus* was purchased from Abcam (catalog Ab20920).

Chromatin immunoprecipitation

Chromatin immunoprecipitation was done as described (Müller et al, 2020). In brief, for chromatin immunoprecipitation, we crosslinked differentiated human keratinocytes with 0.25 M Di(N-succinimidyl) glutarate (DSG) (catalog 20593, Thermo Fisher Scientific) for 45 minutes, followed by washing and 10 minutes of additional crosslinking with 1% paraformaldehyde (catalog 28906, Thermo Fisher Scientific). After chromatin extraction, the chromatin was sonicated for 25 cycles using the Bioruptor (Diagenode). After brief centrifugation for 5 minutes at 13,000 r.p.m. 4 °C, chromatin was subjected to preclearing for removal of *S aureus*−derived Protein A by incubating the chromatin for 1 hour with 2 μg IgG and protein G Dynabeads (catalog 10004, Thermo Fisher Scientific). After preclearing, lysates were incubated with an anti-IκBζ (homemade antibody raised against the IκBζ peptide CRKGADPSTRNLENEQ). After washing, decrosslinking, and purification of the DNA, qPCR was performed using the same conditions described for gene expression analysis but using the Maxima SYBR Green Master Mix (catalog K0221, Thermo Fisher Scientific). Sequences of the chromatin immunoprecipitation primers are found in Supplementary Table S5.

Cytokine array

To analyze the secretion of cytokines in *S aureus*−infected back skin, Proteome Profiler Mouse Cytokine Array Kit Panel A (catalog ARY006, R&D Systems) was applied according to the instructions. In brief, back skin samples were homogenized in gentleMACS C-tubes (catalog 130-093-237, Miltenyi) using the gentleMACS dissociator with protein lysis buffer, lysed for 10 minutes on ice, and further processed as previously described (Fischer et al, 2023). After determination of the protein concentration, samples from 3 mice per group were pooled and analyzed. The development of the membranes was conducted in parallel using the same exposure time at the Fusion FX imager (Peqlab). Subsequently, relative pixel values were obtained using the dot blot analyzer (ImageJ), and values were normalized to the reference spots provided on the membranes.

Flow cytometry

Infiltration of immune cells upon epicutaneous *S aureus* infection was analyzed by flow cytometry using single-cell suspensions from the back skin as described (Fischer et al, 2023). The following antibodies from BioLegend were used for staining: anti-CD4-PE (catalog 100408, clone GK1.5), anti-CD25-APC (catalog 101910, clone 3C7), anti-Ly6G-PE (catalog 127607, clone 1A8), anti-Ly6C-APC (catalog 128016, clone HK1.4), and anti-γδ-APC (catalog 118115, clone GL3). All data were acquired using a LSR II flow cytometer (Becton Dickson), with gate settings based on the respective isotype controls (catalog 400612, APC Rat IgG2b, κ, BioLegend; catalog 400636, PE Rat IgG2b, κ, BioLegend; and catalog 550085, PE Hamster IgG2, κ, Becton Dickson). For live/dead staining, the samples were costained with DAPI (catalog 422801, BioLegend). The gating strategy is presented in Supplementary Figure S2c, with respective cell populations gated on live single cells using the FlowJo (Tree Star) software.

Detection of ROS in skin

Single-cell suspensions (preparation details are provided in flow cytometry section) of each mouse with approximately 5×10^5 cells/ml of the digested skin samples were dissolved in PBS and divided into 3 samples: blank, rested (with DMSO), and phorbol 12-myristate 13-acetate−restimulated cells (0.5 μg/ml, catalog P1585-5MG, Sigma-Aldrich). All samples were incubated for 30 minutes at 37 °C before they were filled up to 1 ml with PBS. An intermediate CellRox Green reagent solution (250 μM in DMSO, catalog C10492, Thermo Fisher Scientific) was prepared according to the manufacturer's instructions and added to rested or phorbol 12-myristate 13-acetate (PMA)−treated cells (final concentration 500 nM); the blank samples received DMSO as a vehicle instead. All samples were incubated for 35 minutes at 37 °C in the dark, whereas live/dead stain SytoxRed was added during the remaining 15-minute incubation time. Flow cytometric measurement was conducted within the next 2 hours using the APC channel for SytoxRed and FITC channel for CellRox detection. For the analysis, ROS-producing cells were gated in comparison with their respective blank samples. The percentage of ROS-producing cells (per gated cells) was calculated using the FlowJo (Tree Star) software.

Immunohistochemistry

Preparation of back skin tissue and staining were done as previously described (Lorscheid et al, 2019). Antigen retrieval was conducted for 40 minutes in 10 mM citrate buffer (pH 6). The following antibodies and dilutions were applied: cleaved caspase-3 (catalog 9664, Cell Signaling Technology, 1:500 diluted) and CD3 (catalog NB600-1441, Novus Biologicals, 1:200 diluted). Antibody staining was further conducted overnight in 5% normal goat serum (catalog 5425S, Cell Signaling Technology) in the presence of 0.1% Triton-X-100.

Confocal immunofluorescence microscopy to assess bacterial infiltration

Formalin-fixed, paraffin-embedded tissue sections from murine back skin were deparaffinized using RotiHistol and a series of ethanol washes. To reverse formaldehyde crosslinks, the sections were boiled in citrate buffer (pH 6.0) for 25 minutes and rinsed 3 times for 5 minutes with PBS. Reduction of nonspecific background signal was achieved by overnight incubation at 4 °C using blocking buffer (10% normal chicken serum in PBS). For staining, the sections were incubated with primary antibodies for 2 hours at room temperature and secondary antibodies for 1 hour at room temperature in the dark. All antibody dilutions were prepared in blocking buffer (anti-protein A antibody, host: rabbit, 1:500, catalog P3775, Sigma-Aldrich; secondary AF594 anti-rabbit antibody, 1:500, catalog A-21442, Thermo Fisher Scientific). For the removal of excessive antibodies, sections were washed 3 times for 5 minutes with PBS after each incubation step. Nuclear DNA staining was conducted using Hoechst 33342 (1 μg/ml, catalog H21492, Thermo Fisher Scientific) in PBS for 10 minutes at room temperature in the dark. The coverslips were washed again, mounted using ProLong Diamond Antifade (catalog P36961, Thermo Fisher Scientific), and dried overnight at room temperature in the dark. Imaging of 6 × 6 tiles was performed with a Zeiss LSM 800 Confocal microscope (Carl Zeiss) using a ×20 objective and Airyscan acquisition. After image acquisition, the data were processed using ImageJ-Win64 software (National Institutes of Health).

Statistical analysis

Obtained results are represented as the mean ± SD (in vitro stimulation) or mean ± SEM (n = animal numbers). Significance levels were calculated using a 2-tailed Student's *t*-test and are depicted with asterisks (*$P < .05$, **$P < .01$, and ***$P < .001$, with ns denoting not significant). All data plots were generated using GraphPad Prism software.

ETHICS STATEMENT

All animal experiments were approved by the local animal ethics committee (G22-1-049, Landesuntersuchungsamt Rheinland-Pfalz) and conducted following German law and guidelines for animal care. Isolation of primary human keratinocytes from foreskin was approved by the local ethics committee of the University Hospital Tübingen. Discarded tissue from circumcision procedures was used.

DATA AVAILABILITY STATEMENT

The datasets produced in this study are available in the following databases: Gene Expression Omnibus GSE46843 for RNA-seq data. Raw data used to generate the heatmaps are further provided in Supplementary Tables S1, S2, and S6.

CONFLICT OF INTEREST

The authors state no conflict of interest.

ACKNOWLEDGMENTS

The study was supported by grants from the Foundation of Experimental Biomedicine (to DK) and the Deutsche Forschungsgemeinschaft, TRR156/3 (project number 246807620, B09, A01, B05) (to DK, BS, and ANRW), TRR355/1 (project number 490846870, A08) (to DK), SFB 1292/2 (project number 318346496, TP08) (to CD), the Deutsche Forschungsgemeinschaft Emmy Noether Program (DE 2654/2-1) (to CD), and SPP2225 (project number We-4195/25-1) (to ANRW). Furthermore, CD is supported by the Federal Ministry of Education and Research (grant number 03ZU1202GA), and DK is supported by the Rise up! programme of the Boehringer Ingelheim Foundation. We thank Claudia Braun from the Histology Core Facility (University Medical Center Mainz, Johannes Gutenberg-University), Bonny Adami (University Medical Center Mainz, Johannes Gutenberg-University), Jule Focken, and Birgit Sauer (Eberhard Karls-University) for experimental support. We also thank Stephan Hailfinger (University Medical Center Münster) for the donation of *NFKBIZ*-encoding plasmids and Christiane Wolz and Bernhard Krismer (both from Eberhard Karls-University) for providing the bacteria. We also thank Ana-Marija Kulis-Mandic for technical assistance.

AUTHOR CONTRIBUTIONS

Conceptualization: BF, DK, MW, BS, ANRW; Formal Analysis: BF, AK, TK, MK, EF, EM, DL, FB, FE, MC, CD; Funding Acquisition: DK; Methodology: BF, AK, TK, MK, EF, EM, DL, FB, FE, MC, CD; Project Administration: DK; Supervision: DK; Writing − Original Draft Preparation: BF, DK, MW, KS-O; Writing - Review and Editing: BF, AK, EF, TK, MK, DL, FB, FE, MC, EM, CD, ANRW, MW, BS, KS-O, DK

SUPPLEMENTARY MATERIAL

Supplementary material is linked to the online version of the paper at www.jidonline.org, and at https://doi.org/10.1016/j.jid.2025.04.036.

REFERENCES

Al Kindi A, Alkahtani AM, Nalubega M, El-Chami C, O'Neill C, Arkwright PD, et al. Staphylococcus aureus internalized by skin keratinocytes evade antibiotic killing. Front Microbiol 2019;10:2242.

Annemann M, Plaza-Sirvent C, Schuster M, Katsoulis-Dimitriou K, Kliche S, Schraven B, et al. Atypical IκB proteins in immune cell differentiation and function. Immunol Lett 2016;171:26−35.

Antimicrobial Resistance Collaborators. Global burden of bacterial antimicrobial resistance in 2019: a systematic analysis [published correction appears in Lancet 2022;400:1102] Lancet 2022;399:629−55.

Askarian F, Wagner T, Johannessen M, Nizet V. Staphylococcus aureus modulation of innate immune responses through Toll-like (TLR), (NOD)-like (NLR) and C-type lectin (CLR) receptors. FEMS Microbiol Rev 2018;42:656−71.

Braff MH, Zaiou M, Fierer J, Nizet V, Gallo RL. Keratinocyte production of cathelicidin provides direct activity against bacterial skin pathogens. Infect Immun 2005;73:6771−81.

Centers for Disease Control and Prevention (CDC). Outbreaks of community-associated methicillin-resistant staphylococcus aureus skin infections–Los Angeles County, California, 2002-2003. MMWR Morb Mortal Wkly Rep 2003;52:88.

Del Giudice P. Skin infections caused by Staphylococcus aureus. Acta Derm Venereol 2020;100:adv00110.

Evangelista JE, Xie Z, Marino GB, Nguyen N, Clarke DJB, Ma'ayan A. Enrichr-KG: bridging enrichment analysis across multiple libraries. Nucleic Acids Res 2023;51:W168−79.

Fischer B, Kübelbeck T, Kolb A, Ringen J, Waisman A, Wittmann M, et al. IL-17A-driven psoriasis is critically dependent on IL-36 signaling. Front Immunol 2023;14:1256133.

Gimenez-Rivera VA, Patel H, Dupuy FP, Allakhverdi Z, Bouchard C, Madrenas J, et al. NOD2 agonism counter-regulates human Type 2 T cell functions in peripheral blood mononuclear cell cultures: implications for atopic dermatitis. Biomolecules 2023;13:369.

Grimes CL, Ariyananda Lde Z, Melnyk JE, O'Shea EK. The innate immune protein Nod2 binds directly to MDP, a bacterial cell wall fragment. J Am Chem Soc 2012;134:13535−7.

Hanzelmann D, Joo HS, Franz-Wachtel M, Hertlein T, Stevanovic S, Macek B, et al. Toll-like receptor 2 activation depends on lipopeptide shedding by bacterial surfactants. Nat Commun 2016;7:12304.

Hashimoto M, Tawaratsumida K, Kariya H, Aoyama K, Tamura T, Suda Y. Lipoprotein is a predominant toll-like receptor 2 ligand in Staphylococcus aureus cell wall components. Int Immunol 2006;18:355−62.

Hildebrand DG, Alexander E, Hörber S, Lehle S, Obermayer K, Münck NA, et al. IκBζ is a transcriptional key regulator of CCL2/MCP-1. J Immunol 2013;190:4812−20.

Hruz P, Zinkernagel AS, Jenikova G, Botwin GJ, Hugot JP, Karin M, et al. NOD2 contributes to cutaneous defense against Staphylococcus aureus through alpha-toxin-dependent innate immune activation. Proc Natl Acad Sci USA 2009;106:12873−8.

Jevon M, Guo C, Ma B, Mordan N, Nair SP, Harris M, et al. Mechanisms of internalization of Staphylococcus aureus by cultured human osteoblasts. Infect Immun 1999;67:2677−81.

Jiao D, Wong CK, Qiu HN, Dong J, Cai Z, Chu M, et al. NOD2 and TLR2 ligands trigger the activation of basophils and eosinophils by interacting

with dermal fibroblasts in atopic dermatitis-like skin inflammation. Cell Mol Immunol 2016;13:535–50.

Johansen C, Mose M, Bertelsen T, Vinter H, Lorscheid S, Schulze-Osthoff K, et al. The I kappa B zeta protein is a downstream target of interleukin-17A and a key driver in the development of psoriasis. Brit J Dermatol 2014;171. E107-E.

Johansen C, Mose M, Ommen P, Bertelsen T, Vinter H, Hailfinger S, et al. IκBζ is a key driver in the development of psoriasis. Proc Natl Acad Sci USA 2015;112:E5825–33.

Kabesch M, Peters W, Carr D, Leupold W, Weiland SK, von Mutius E. Association between polymorphisms in caspase recruitment domain containing protein 15 and allergy in two German populations. J Allergy Clin Immunol 2003;111:813–7.

Kayama H, Ramirez-Carrozzi VR, Yamamoto M, Mizutani T, Kuwata H, Iba H, et al. Class-specific regulation of pro-inflammatory genes by MyD88 pathways and IkappaBzeta. J Biol Chem 2008;283:12468–77.

Kim Y, Lee YS, Yang JY, Lee SH, Park YY, Kweon MN. The resident pathobiont Staphylococcus xylosus in Nfkbiz-deficient skin accelerates spontaneous skin inflammation. Sci Rep 2017;7:6348.

Lai Y, Cogen AL, Radek KA, Park HJ, Macleod DT, Leichtle A, et al. Activation of TLR2 by a small molecule produced by staphylococcus epidermidis increases antimicrobial defense against bacterial skin infections. J Invest Dermatol 2010;130:2211–21.

Liu H, Archer NK, Dillen CA, Wang Y, Ashbaugh AG, Ortines RV, et al. Staphylococcus aureus epicutaneous exposure drives skin inflammation via IL-36-Mediated T cell responses. Cell Host Microbe 2017;22:653–66.e5.

Lorenz E, Mira JP, Cornish KL, Arbour NC, Schwartz DA. A novel polymorphism in the toll-like receptor 2 gene and its potential association with staphylococcal infection. Infect Immun 2000;68:6398–401.

Lorscheid S, Müller A, Löffler J, Resch C, Bucher P, Kurschus FC, et al. Keratinocyte-derived IκBζ drives psoriasis and associated systemic inflammation. JCI Insight 2019;4:e130835.

Macaluso F, Nothnagel M, Parwez Q, Petrasch-Parwez E, Bechara FG, Epplen JT, et al. Polymorphisms in NACHT-LRR (NLR) genes in atopic dermatitis. Exp Dermatol 2007;16:692–8.

Macleod T, Ainscough JS, Hesse C, Konzok S, Braun A, Buhl AL, et al. The proinflammatory cytokine IL-36γ is a global discriminator of harmless microbes and invasive pathogens within epithelial tissues. Cell Rep 2020;33:108515.

Miller LG, Perdreau-Remington F, Rieg G, Mehdi S, Perlroth J, Bayer AS, et al. Necrotizing fasciitis caused by community-associated methicillin-resistant Staphylococcus aureus in los Angeles. N Engl J Med 2005;352:1445–53.

Miller LS, O'Connell RM, Gutierrez MA, Pietras EM, Shahangian A, Gross CE, et al. MyD88 mediates neutrophil recruitment initiated by IL-1R but not TLR2 activation in immunity against Staphylococcus aureus. Immunity 2006;24:79–91.

Moos S, Regen T, Wanke F, Tian Y, Arendholz LT, Hauptmann J, et al. IL-17 signaling in keratinocytes orchestrates the defense against Staphylococcus aureus skin infection. J Invest Dermatol 2023;143:1257–67.e10.

Müller A, Dickmanns A, Resch C, Schäkel K, Hailfinger S, Dobbelstein M, et al. The CDK4/6-EZH2 pathway is a potential therapeutic target for psoriasis. J Clin Invest 2020;130:5765–81.

Müller A, Hennig A, Lorscheid S, Grondona P, Schulze-Osthoff K, Hailfinger S, et al. IκBζ is a key transcriptional regulator of IL-36-driven psoriasis-related gene expression in keratinocytes. Proc Natl Acad Sci USA 2018;115:10088–93.

Nakatsuji T, Chen TH, Two AM, Chun KA, Narala S, Geha RS, et al. Staphylococcus aureus exploits epidermal barrier defects in atopic dermatitis to trigger cytokine expression. J Invest Dermatol 2016;136:2192–200.

Negroni A, Pierdomenico M, Cucchiara S, Stronati L. NOD2 and inflammation: current insights. J Inflamm Res 2018;11:49–60.

Ngo QV, Faass L, Sähr A, Hildebrand D, Eigenbrod T, Heeg K, et al. Inflammatory response against staphylococcus aureus via intracellular sensing of nucleic acids in keratinocytes [published correction appears in Front Immunol 2024;15:1330357]. Front Immunol 2022;13:828626.

Ogura Y, Bonen DK, Inohara N, Nicolae DL, Chen FF, Ramos R, et al. A frameshift mutation in NOD2 associated with susceptibility to Crohn's disease. Nature 2001;411:603–6.

Ong PY, Ohtake T, Brandt C, Strickland I, Boguniewicz M, Ganz T, et al. Endogenous antimicrobial peptides and skin infections in atopic dermatitis. N Engl J Med 2002;347:1151–60.

Patrick GJ, Liu H, Alphonse MP, Dikeman DA, Youn C, Otterson JC, et al. Epicutaneous Staphylococcus aureus induces IL-36 to enhance IgE production and ensuing allergic disease. J Clin Invest 2021;131: e143334.

Roth SA, Simanski M, Rademacher F, Schröder L, Harder J. The pattern recognition receptor NOD2 mediates Staphylococcus aureus-induced IL-17C expression in keratinocytes. J Invest Dermatol 2014;134:374–80.

Shoaib M, Aqib AI, Muzammil I, Majeed N, Bhutta ZA, Kulyar MF, et al. MRSA compendium of epidemiology, transmission, pathophysiology, treatment, and prevention within one health framework. Front Microbiol 2022;13:1067284.

Sidiq T, Yoshihama S, Downs I, Kobayashi KS. Nod2: a critical regulator of ileal microbiota and Crohn's disease. Front Immunol 2016;7:367.

Siegmund A, Afzal MA, Tetzlaff F, Keinhörster D, Gratani F, Paprotka K, et al. Intracellular persistence of Staphylococcus aureus in endothelial cells is promoted by the absence of phenol-soluble modulins. Virulence 2021;12: 1186–98.

Simanski M, Dressel S, Gläser R, Harder J. RNase 7 protects healthy skin from Staphylococcus aureus colonization. J Invest Dermatol 2010;130:2836–8.

Stroo I, Butter LM, Claessen N, Teske GJ, Rubino SJ, Girardin SE, et al. Phenotyping of Nod1/2 double deficient mice and characterization of Nod1/2 in systemic inflammation and associated renal disease. Biol Open 2012;1: 1239–47.

Takeuchi O, Hoshino K, Akira S. Cutting edge: TLR2-deficient and MyD88-deficient mice are highly susceptible to Staphylococcus aureus infection. J Immunol 2000;165:5392–6.

Tartey S, Matsushita K, Vandenbon A, Ori D, Imamura T, Mino T, et al. Akirin2 is critical for inducing inflammatory genes by bridging IκB-ζ and the SWI/SNF complex. EMBO J 2014;33:2332–48.

Tenover FC, Goering RV. Methicillin-resistant Staphylococcus aureus strain USA300: origin and epidemiology. J Antimicrob Chemother 2009;64: 441–6.

Terui H, Yamasaki K, Wada-Irimada M, Onodera-Amagai M, Hatchome N, Mizuashi M, et al. Staphylococcus aureus skin colonization promotes SLE-like autoimmune inflammation via neutrophil activation and the IL-23/IL-17 axis. Sci Immunol 2022;7:eabm9811.

Thurlow LR, Joshi GS, Richardson AR. Virulence strategies of the dominant USA300 lineage of community-associated methicillin-resistant Staphylococcus aureus (CA-MRSA). FEMS Immunol Med Microbiol 2012;65:5–22.

Voss E, Wehkamp J, Wehkamp K, Stange EF, Schröder JM, Harder J. NOD2/CARD15 mediates induction of the antimicrobial peptide human beta-defensin-2. J Biol Chem 2006;281:2005–11.

Williams H, Crompton RA, Thomason HA, Campbell L, Singh G, McBain AJ, et al. Cutaneous Nod2 expression regulates the skin microbiome and wound healing in a murine model. J Invest Dermatol 2017;137:2427–36.

Yamamoto M, Yamazaki S, Uematsu S, Sato S, Hemmi H, Hoshino K, et al. Regulation of Toll/IL-1-receptor-mediated gene expression by the inducible nuclear protein IkappaBzeta. Nature 2004;430:218–22.

This work is licensed under a Creative Commons Attribution 4.0 International License. To view a copy of this license, visit http://creativecommons.org/licenses/by/4.0/

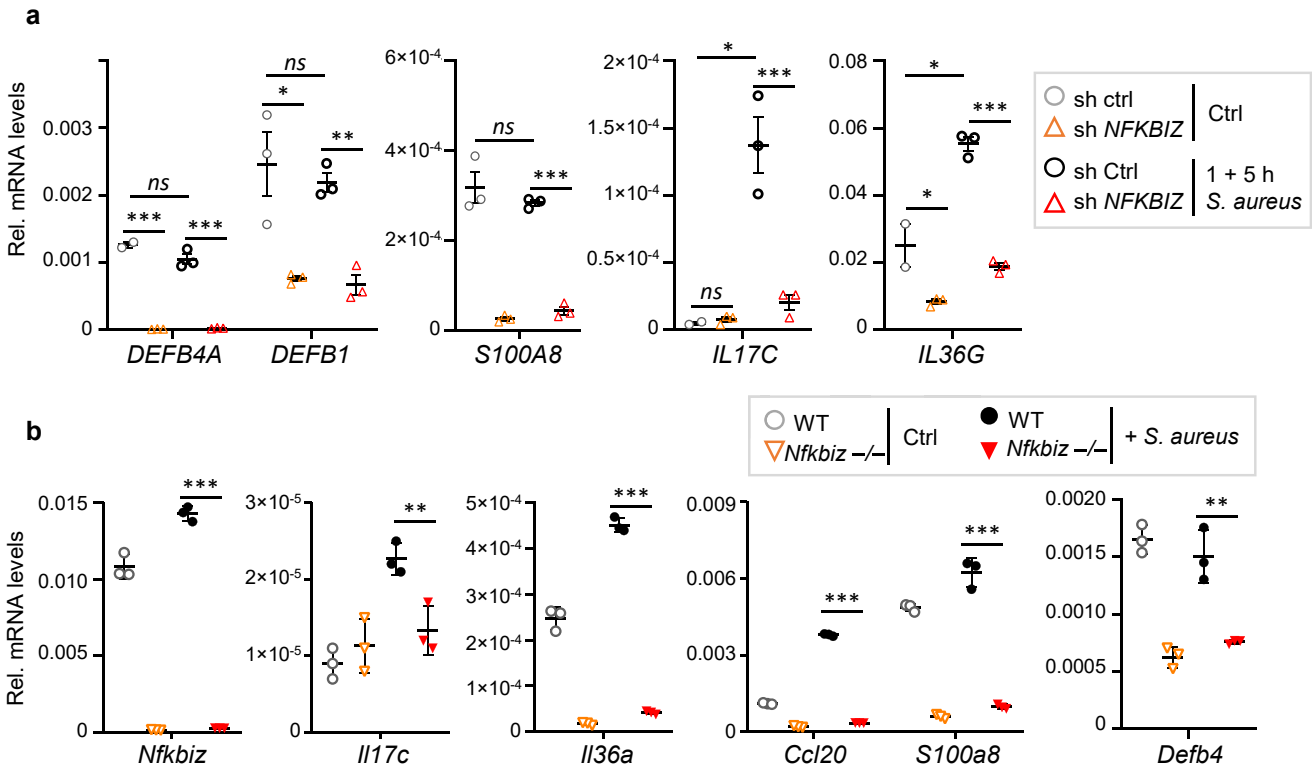

Supplementary Figure S1. Further gene expression analysis of *Nfkbiz* target genes in *S aureus*–infected human and murine keratinocytes. (**a**) Relative mRNA expression levels of IκBζ target genes from control and *NFKBIZ*-depleted primary human keratinocytes 6 h (1 h infection, 5 h further incubation) after *S aureus* infection. Values were normalized to the reference gene *RPL37A* to calculate the relative mRNA levels. Shown is the mean of 3 biological replicates ± SD. (**b**) Gene expression in WT and *Nfkbiz*-knockout (*Nfkbiz*-/-) murine keratinocytes analyzed 24 h after 1 h of infection with *S aureus*. Relative mRNA levels were normalized to *Actb*. Samples from 2−3 mice per group were pooled before analysis. Significance was calculated using a 2-tailed Student's *t*-test (*$P < .05$, **$P < .01$, and ***$P < .001$). h, hour; ns, not significant; WT, wild-type.

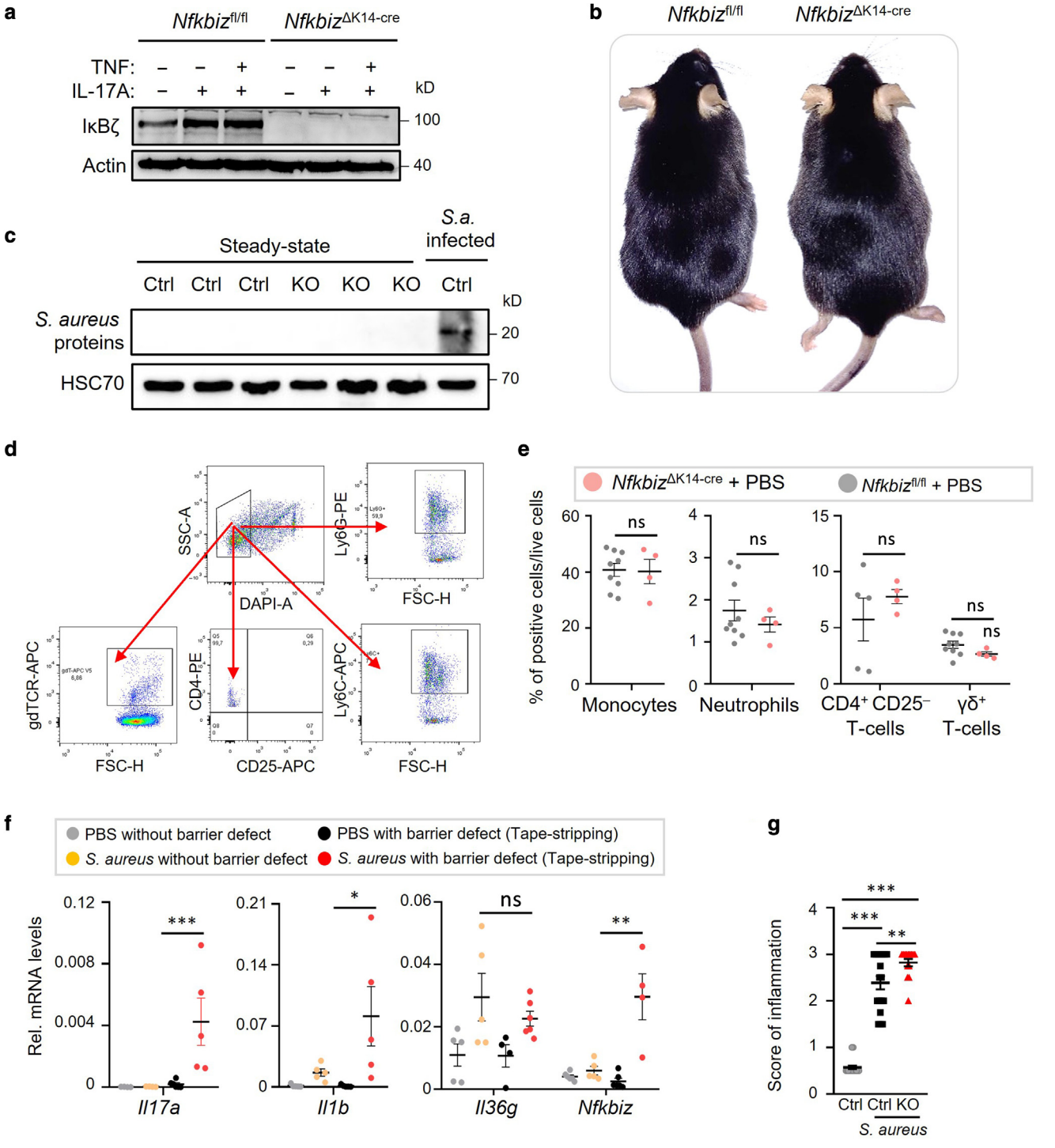

Supplementary Figure S2. Steady-state analysis of NfkbizΔK14-cre mice and inflammation-promoting effects upon mild barrier disruption. (**a**) Immunoblot analysis of IκBζ expression in untreated and IL-17A (100 ng/ml) or IL-17A and TNF (10 ng/ml)-treated murine keratinocytes after 1 h of treatment. Keratinocytes were isolated from the tails of *Nfkbiz*$^{fl/fl}$ control or *Nfkbiz*$^{\Delta K14\text{-}cre}$ mice. Actin served as control for equal loading. (**b**) Visual controls of the skin of adult *Nfkbiz*$^{fl/fl}$ and *Nfkbiz*$^{\Delta K14\text{-}cre}$ mice (aged >37 weeks). (**c**) Immunoblot of *S aureus* protein using skin lysates of PBS-treated *Nfkbiz*$^{fl/fl}$ and *Nfkbiz*$^{\Delta K14\text{-}cre}$ mice compared with that of *S aureus*–infected control lysate. HSC70 served as a loading control. (**d**) FACS gating strategy of back skin cells from *S aureus*–infected *Nfkbiz*$^{fl/fl}$ and *Nfkbiz*$^{\Delta K14\text{-}cre}$ mice. The immune cell populations gated on living single cells and respective stainings were evaluated using FlowJo (Tree Star) software. (**e**) Flow cytometry analysis of skin-infiltrating immune cells from the the back skin of 7-day PBS-treated *Nfkbiz*$^{fl/fl}$ and *Nfkbiz*$^{\Delta K14\text{-}cre}$ mice. Shown is the mean ± SEM (n = 4–10 mice per group) of the relative percentage of positive live cells. Neutrophils = Ly6G$^+$, monocytes = Ly6C$^+$, effector CD4$^+$ T cells = CD4$^+$ CD25$^-$, and γδ T cells = γδ-TCR$^+$. (**f**)Gene expression analysis of wild-type mice, which were subjected to epicutaneous *S aureus* infection either after shaving of the back skin (without barrier defect) or after shaving, depilation, and tape stripping of the skin before infection. In both applications, equal amounts of living bacteria were applied on the back skin, covered for 7 days, and subsequently analyzed by qPCR. Relative mRNA levels were normalized to *Actb*. Shown is the mean ± SEM (n = 4–6 mice per group). (**g**) Score for the severity of inflammation in the back skin on day 7 in PBS-treated control mice (gray dots), *S aureus*–infected *Nfkbiz*$^{fl/fl}$ (black dots) mice, and *Nfkbiz*$^{\Delta K14\text{-}cre}$ (red dots) mice. Significance was calculated using a 2-tailed Student's *t*-test (*$P < .05$, **$P < .01$, and ***$P < .001$). FSC-H, forward scatter height; h, hour; ns, not significant; SCC-A, side scatter area.

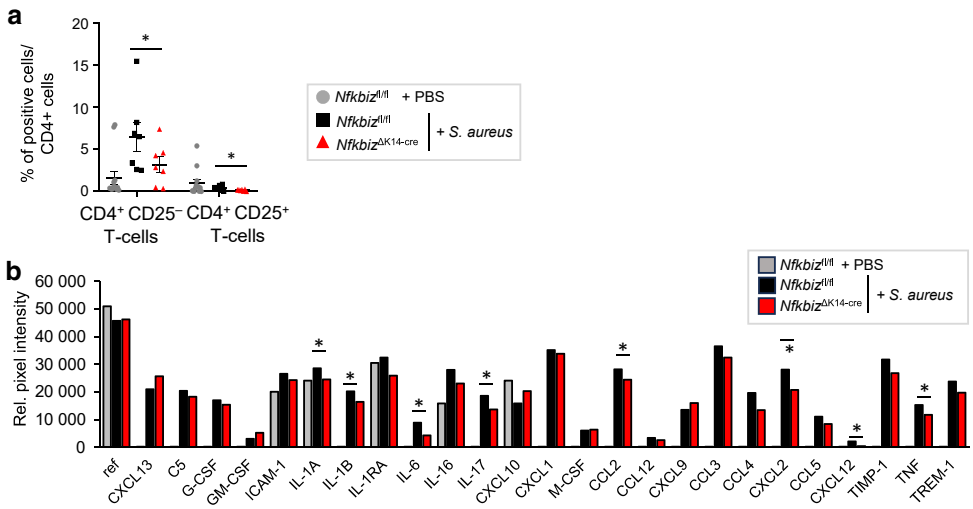

Supplementary Figure S3. Additional data of control and *Nfkbiz*$^{\Delta K14\text{-}cre}$ mice after epicutaneous infection with *S aureus*. (**a**) Flow cytometry analysis of skin-infiltrating CD4$^+$ T cells and regulatory (CD4$^+$ CD25$^+$) T cells from PBS-treated control and *S aureus*–infected *Nfkbiz*$^{fl/fl}$ and *Nfkbiz*$^{\Delta K14\text{-}cre}$ mice 7 days after infection. Shown is the relative percentage of positive live cells after pregating on viable CD4$^+$ T cells. Shown is the mean ± SEM (n = 7–13 mice per group). (**b**) Protein levels of cytokines and chemokines from control and infected *Nfkbiz*$^{fl/fl}$ or *Nfkbiz*$^{\Delta K14\text{-}cre}$ mice 7 days after infection. Shown are results normalized to the reference controls and depicted as relative pixel values. Samples from 4 mice per group were pooled before analysis. Significance was calculated using a 2-tailed Student's *t*-test (*$P < .05$).

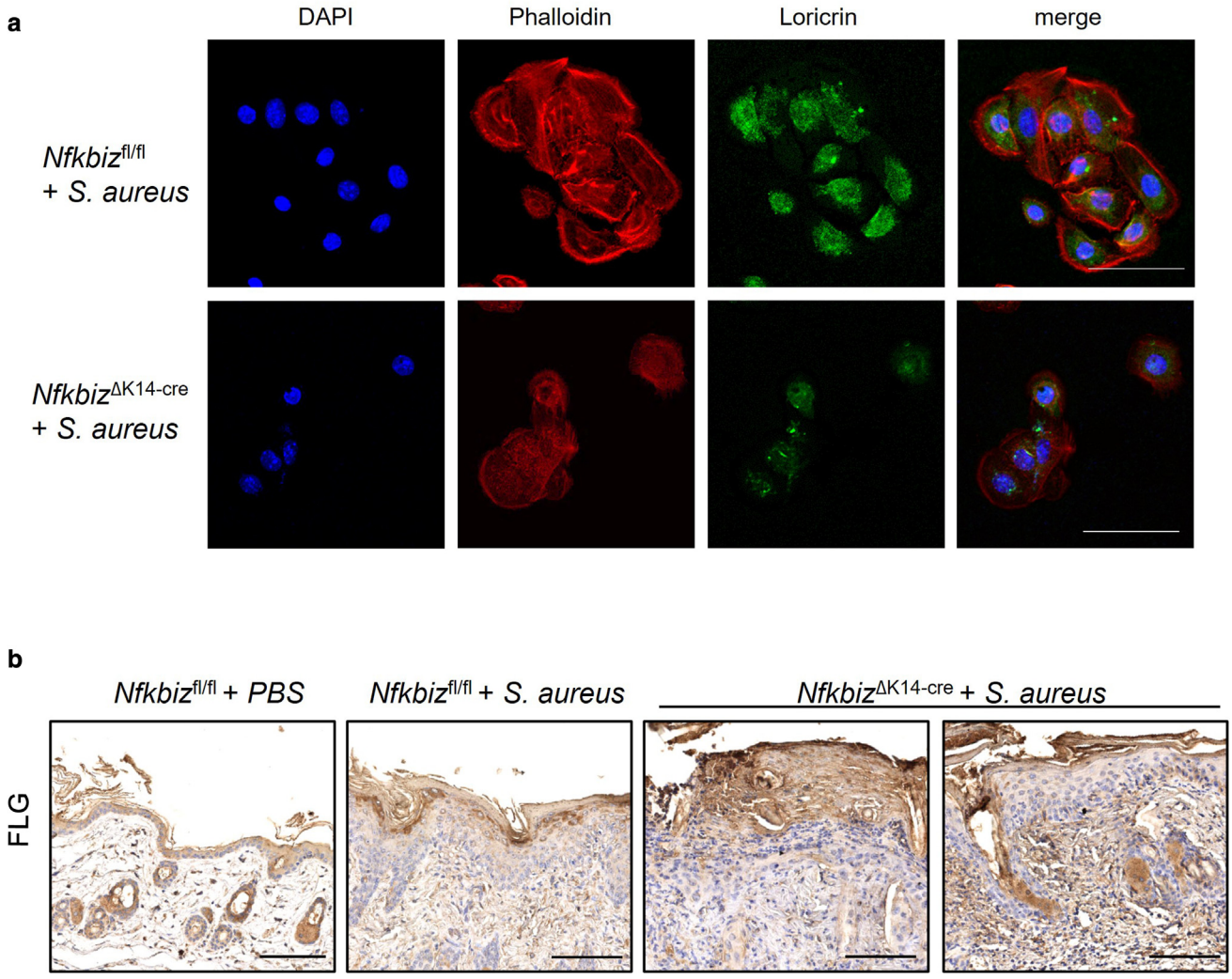

Supplementary Figure S4. Analysis of the expression of skin barrier proteins upon deletion of IκBζ from *S aureus*–infected keratinocytes or skin. (**a**) Immunofluorescence staining of the actin cytoskeleton (red) and loricrin (green) in *S aureus*–infected control and *Nfkbiz*-KO (*Nfkbiz*$^{\Delta K14\text{-cre}}$) mouse keratinocytes. Cells were infected for 1 h, followed by an additional incubation time of 23 h. Nuclei were stained with Hoechst (blue). Bar = 50 μm. (**b**) FLG staining of the skin from PBS-treated control and *S aureus*–infected *Nfkbiz*$^{fl/fl}$ and *Nfkbiz*$^{\Delta K14\text{-cre}}$ mice 7 days after infection. Bars = 100 μm. h, hour; KO, knockout.

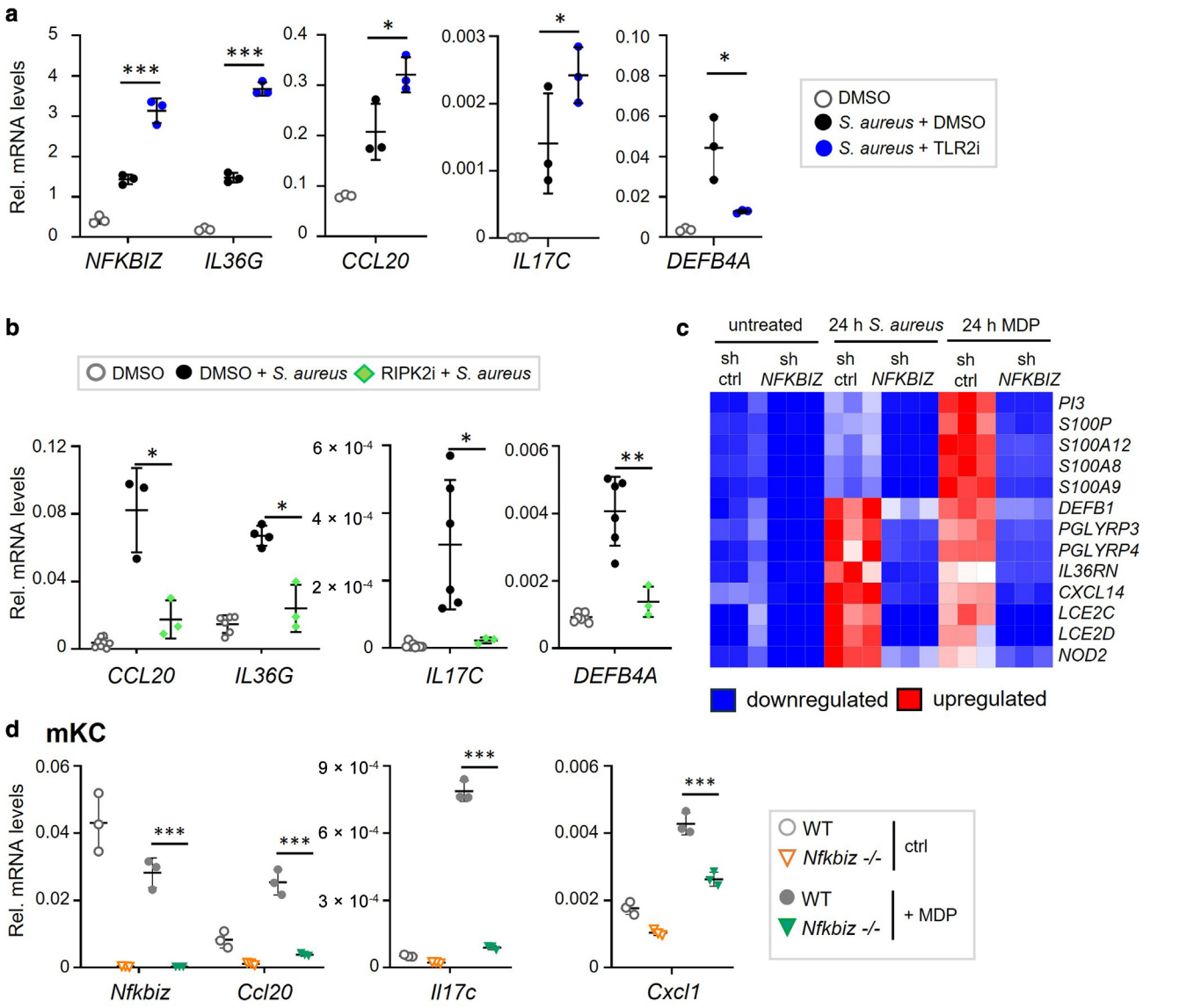

Supplementary Figure S5. Additional data on NOD2, TLR2, and IκBζ signaling in response to *S aureus* infection or MDP stimulation. (**a**) Gene expression analysis of primary human keratinocytes treated for 1 h with *S aureus* in the presence or absence of DMSO as vehicle control or 50 μM of the TLR2i C29. Cells were harvested 24 h after infection. Relative mRNA levels were calculated over the *U6RNA* reference gene. (**b**) Similar experiment as in **a** using 5 μM RIPK2i GSK583 instead of TLR2i. (**c**) Heatmap of selected IκBζ target genes encoding antimicrobial peptides and proteins involved in barrier formation, differentiation, or downstream targets of IL-17 and IL-36 (full heatmap is provided in Supplementary Figure S6). **(d)** Gene expression analysis of control and *Nfkbiz*-depleted murine keratinocytes, transfected and stimulated for 1 h with MDP. Relative mRNA levels were normalized over *Actb*. Significance was calculated using a 2-tailed Student's *t*-test (**P* < .05, ***P* < .01, and ****P* < .001). h, hour; MDP, muramyl dipeptide; ns, not significant; RIPK2i, RIPK2 inhibitor; TLR2, toll-like receptor 2; TLR2i, toll-like receptor 2 inhibitor.

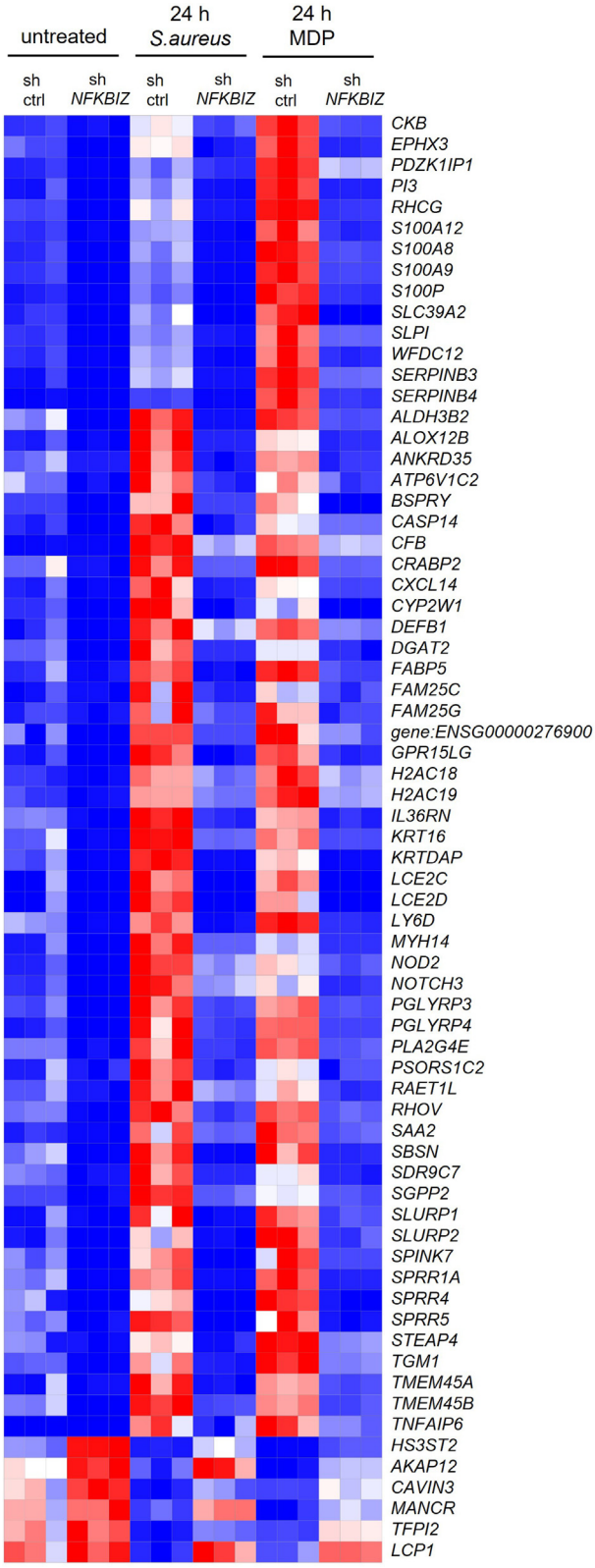

Supplementary Figure S6. IκBζ target genes in MDP-treated keratinocytes. Presented is a heatmap of all 69 significantly regulated IκBζ-dependent target genes overlapping after 24 h of *S aureus* infection or MDP stimulation (cut off: $P \leq .05$, fold change absolute > 2, difference absolute > 3). MDP, muramyl dipeptide.